AN ABSTRACT OF THE THESIS OF

Taylor Mellon for the degree of Master of Science in Mechanical Engineering presented on August 24, 2021.

Title: Using Digital Human Modeling to Evaluate and Improve Car Pillar Design: A Proof of Concept and Design of Experiments

Abstract approved: _____

H. Onan Demirel

Considering human factors in early engineering design stages can improve expensive late stage processes, facilitate user safety, improve product quality and help reduce the need for physical prototyping. Currently, car pillar design (the vertical pillars between windows which connect the roof and car body) provide safety for the passengers in case of a rollover accident. However, these pillars are known to cause accidents because of the vision they obstruct or limit. Literature suggests solutions to this problem by changing the position, geometry and using cameras for an augmented display but these can be expensive, not eliminate the obstruction zone or may require extensive physical prototyping. This research suggests a methodology to analyze and improve vision obstruction through by integrating Computer Aided Design Models (CAD) and JAck Digital Human Modeling (DHM) Software. This research then provides greater evidence through a Design of Experiments to compare different car pillar designs for percent area visible. The results conclude that this is a valuable method to test the amount of vision be obstructed by the pillars. Additionally, the research concludes that provide cuts within the car pillar geometry can provide increased visibility. The results include; four car models, four traffic scenes, six driver anthropometries, four pedestrian anthropometries, percent area of vision obstruction values, generalized Finite Element Analysis (FEA) of pillar designs and statistical models and analyses to prove significance of the car pillar improvements.

Using Digital Human Modeling to Evaluate and Improve Car Pillar Design: A Proof of Concept and Design of Experiments

by

Taylor Mellon

A THESIS

submitted to

Oregon State University

in partial fulfillment of
the requirements for the
degree of

Master of Science

Presented August 24, 2021
Commencement June 2022

Master of Science thesis of Taylor Mellon presented on August 24, 2021.

APPROVED:

Major Professor, representing Mechanical Engineering

Head of the School of Mechanical, Industrial, and Manufacturing Engineering

---

Dean of the Graduate School

I understand that my thesis will become part of the permanent collection of Oregon State University libraries. My signature below authorizes release of my thesis to any reader upon request.

Taylor Mellon, Author

ACKNOWLEDGEMENTS

The author expresses sincere appreciation for this exciting research opportunity. Thank you Dr. H. Onan Demirel, Dr. Christopher Hoyle, Dr. Matthew Campbell, and the Engineering Design Lab for your collaboration, guidance, patience, and support throughout this master's research. I am grateful for this research opportunity made possible by the MIME faculty and staff.

TABLE OF CONTENTS

TABLE OF CONTENTS (Continued)

Page

LIST OF FIGURES

LIST OF TABLES

Chapter 1: Introduction

This thesis investigates the proof of concept of using Computer Aided Design (CAD) paired with digital human modeling (DHM) in early car pillar design to quantify the percent area of visibility of a target plane which represents a pedestrian. This concept may be used to help quantify different car pillar designs without the need of costly physical prototypes. Additionally, this thesis uses a Design of Experiments (DoE) to further this understanding by providing cuts in these car pillars in the hopes of improving percent area of visibility.

This proof of concept integrates CAD and DHM to incorporate a rudimentary structural analysis and ergonomics analysis to the early concept development or design evaluation phase. This methodology and DoE are to quantify percent area of an obstruction zone based on binocular vison using JACK a DHM tool. This proof of concept and experiment uses four different cars, four separate pillar designs, six different driver anthropometries and four different pedestrian anthropometries. Full scale models of each of the cars used, sports car, sedan, SUV and pickup truck. These models are based on vehicle blue prints and preexisting surface models found on GrabCAD and other online sources [1–4]. The proof of concept includes a brief case study to show how using DHM can quantify percent area of an obstruction zone. Additionally, this includes a rudimentary structural analysis of the pillar designs used on the sports car A-pillar (because it only has four pillars and would experience the most force) to make sure they meet or are close to the roof crash test FMVSS standards. With the concept being proved a full DoE was done with a Kruskal Wallis test to measure whether design variables (cuts in pillars) have significant effects on visual obstructions.

Car pillars are the vertical supports of the windows which connects and provides structural support to roof and the body of the car. These are designated as A, B, C or D pillars respectively working from the front of the car to the back of the car [5]. These car pillars provide a crucial role in the car's aerodynamics, driving dynamics, and, most importantly, passenger safety by protecting drivers from harm in the event of a car crash or rollover. With safety increasing in importance for car design, car pillars have

been getting thicker to provide a higher factor of safety for structural support and to allow for air bagels and other features to be placed within the pillars [5]. However, with the car pillar thickening the visibility of the driver becomes more limited. Literature suggests that traditional car pillars designs obstruct the vision of a driver [6]. This also can be seen in accident reports where the driver "looked but failed to see" a pedestrian walking across the street, pedestrian on a bike or other drivers [7]. Literature has briefly examined the issue of car pillar obscuration and some state-of-the-art solutions have been suggested to solve or mitigate this issue. Some of these solutions involve using cameras with integrated displays, changing pillar position and changing pillar geometry [8–10]. However, these solutions have proven to be costly and require extensive physical prototyping.

The prototyping stage in the engineering design process can be an expensive and extensive process. Additionally, testing different designs and making design changes can be difficult with physical prototypes especially with the vehicle design industry. Computational models used in the early design stages has proven to be a valid method to test and iterate designs [11]. Pairing the computational methods of CAD and DHM in early design stages is becoming more popular as literature suggests it is a valid method for testing and validating designs for ergonomic factors like reach, comfort and visibility (visibility obscuration) [12].

This research investigates a methodology for testing and quantifying car pillar vision obscuration based on binocular vision using CAD integrated with DHM. Additionally, this research investigates different pillar designs on different cars and different scenes to quantify if car pillar visibility can be improved using cuts made in the pillar to create see-through car pillars.

Chapter 2: Obscuration Analysis of Car Pillars Using Digital Human Modeling: A Proof Of Concept

2.1 Abstract

Many automobile accidents involving pedestrians in city driving at roundabouts, intersections, and crossings are related to blind spots, where the driver looked but failed to see the traffic due to the vision obstruction caused by the pillars—vertical posts that tie the body of the car to the roof. Literature has addressed this by suggesting using cameras with integrated displays, changing the position of pillars, or modifying vehicle geometry. However, these solutions can be expensive due to the overall design changes needed and still do not eliminate the obstruction caused by the pillar geometry. This paper provides a proof-of-concept digital prototyping methodology based on digital human modeling (DHM) research that explores A- and D-pillar vision obstructions and introduces an alternative approach to human subject data collection and physical prototyping. This study replicates typical driving conditions by creating a simulation environment that includes two different traffic scenes, two cars, four pillar designs with geometric cuts (see-through pillars), six driver anthropometries, and four pedestrian anthropometries. Overall, the objective of this research is twofold (1) to perform coverage zone analyses to assess the percent area visible of the pedestrian and (2) computationally evaluate the performance of traditional and see-through pillar designs in terms of improvements in forward (A-pillar) and rear (D-pillar) blind spots. The results show that pillar cuts improve the driver's visibility up to 54.46 percent without compromising the Federal Motor Vehicle Safety Standards (FMVSS) 216 roof crush standards.

2.2 Introduction

In 2018, 6,283 pedestrians were killed by a vehicle, and in those reports, drivers claimed that they had checked for pedestrians but failed to see them. After accident investigation and scene reenactment, it was found that a large number of drivers failed to see the

pedestrians because of the obstruction caused by the A-pillar [6]. Automobile pillars are a crucial part of vehicle design due to their contribution to aerodynamics, driving dynamics, and, most importantly, passenger safety by protecting drivers from harm in the event of a car crash or rollover. However, the literature shows that automobile pillars have a negative effect on visibility by causing vision obstruction and not allowing drivers to assess their surroundings properly. For example, Ford has spent an average of 7.5 billion dollars on research and development on their cars in the past four years. Yet, there has been little to no change in the pillar design besides structural changes, like material selection and manufacturing [13]. This paper provides a proof-of-concept digital prototyping methodology based on digital human modeling (DHM) research that explores A- and D-pillar vision obstructions and introduces an alternative cost-effective approach to human subject data collection and physical prototyping. DHM has been largely used in the early stages of product design, mainly assessing the ergonomics of a product. The methodology proposed in this paper enables designers to quantify drivers' visibility for a combination of different conditions, including pedestrians, automobiles, and anthropometries. The case study presented in this paper aims to analyze and compare the vision obscuration of current car pillars and suggests improvements via a see-through pillar design that includes pillars with different geometric cuts. Finally, the impact of the geometric cuts on the structural integrity is assessed via a low-fidelity finite element analysis (FEA) study based on the FMVSS 216 roof crash test standards.

2.3 Literature Review and Background

Before addressing the computational prototyping design approach introduced in this proof-of-concept study, a brief background is provided to highlight the visual obstruction of vehicles, current research that focuses on the problem, and examples showing implementations of DHM in early engineering design.

2.3.1 Vision in Driving

Since drivers are often only on the lookout for other cars in surrounding road traffic, they can easily miss pedestrians, cyclists, vehicles approaching from unexpected directions, road elements, and obstacles. Prior research shows that although drivers may look in

the direction of obstacles, they sometimes fail to see them [14]. These cognitive errors are a cause of late detection in vehicular collisions and can be attributed to human focus being very selective [14]. Perceptual detection errors are categorized as the failure to detect vehicles due to impaired vision from one's periphery in conditions like insufficient lighting [15]. Binocular vision is sight from both eyes combined and has a significant effect on obscuration caused by objects nearby [13].

The position of a driver's head affects what region of their field of view is obstructed. Head position can differ between drivers of different anthropometries as their height and the individual adjustment for seat comfort varies. Without adjustable seats, shorter drivers in a study experienced 3% more blind spot regions while their taller counterparts experienced only about a 1% [16]. Like many automobile components such as mirrors, dashboards, and steering wheels, pillars have been a major element that causes blind spot regions (vision obscuration), leading to automotive collisions. Pillars are the vertical supports on vehicles, often with two around the windshield (A-pillar), between the doors (B- and C- pillars), and two around the back glass (D-pillar). Manufacturers have increased A-pillar thickness and pillar rake angles to improve structural integrity and aerodynamic performance in the last decade [6]. Any pillar that exceeds the width between the driver's eyes obscures a significant portion (Obscuration angle) of the road ahead and any obstacles, vehicles, motorists, or pedestrians in their path [13]. This can be seen in figure 2.1 below. Likewise, slopped or slanted windshield designs implemented to decrease further drag coefficient create additional forward blind spots. Overall, increasing A-pillar width and placement away from straight-ahead increase the chances of lane-change crashes [17, 18] and visual obscuration in turning [19].

2.3.2 Potential Solution to Pillar Obstruction Issue

The problem of car pillars causing a problem for drivers is not a novel concept in research. Currently, there is quite a few state-of-the-art technologies and solutions. This section lists some of these technologies and solutions that are seen in literature. These will include the most common practices used for pillar design and the vision obstruction they cause.

Traditional and Past solutions Traditional solutions to the problem of vision being obstructed by car pillars was to change the position of car to make the view of the

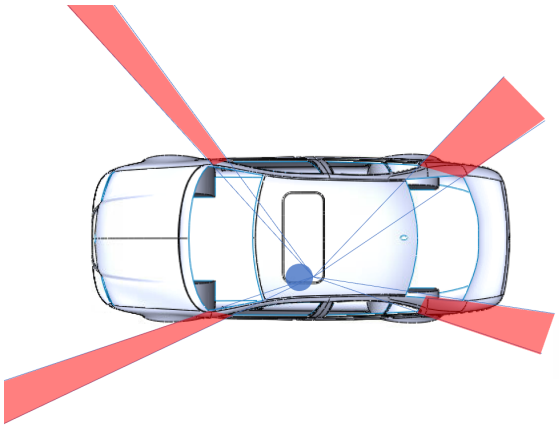

Figure 2.1: Car Pillar Obstructions

driver wider or out of the "main problem points" [20]. Additional traditional ways that this problem has been handled was using thin pillars to minimize the obstruction angle and to split the pillar to provide gaps [6].

Image projection onto pillar: Using camera technology and projecting images of the obscured regions onto the interior of the pillar has been an explored solution. Potential visual differences in color and appearance of the projected images versus the actual environment could cause an added distraction to drivers [8, 21].

Birds-eye view camera: Birds-eye view cameras serve as an added assistance to drivers that do not camouflage the pillar. This system captures and stitches together images from various cameras on the vehicle. The vehicle and surrounding obstacles on the road can be viewed on an in-screen display. This technology has been implemented in cars like the Mitsubishi Pajero and some Nissan vehicles [9, 16].

Geometric cutouts from pillars: Lattice-like cutouts in A-pillars can increase visibility while maintaining necessary pillar strength [8]. The Insurance Institute for Highway Safety (IIHS) requires vehicles to be able withstand four times its weight before the roof crushes 127 mm (5 inches). The National Highway Traffic Safety Administration's 2016 Federal Motor Vehicle Safety Standard requires that vehicles must withstand three times its weight. Inner pillars must also abide by the federal head-impact standards that require foam or other soft material to be used if a passenger collides with it [10]. This has prevented see-through, plexiglass style designs from making it past the concept stage

in the past [22].

2.3.3 Designing with Digital Human Models

Implementing design thinking and human-centered design (HCD) has been a growing interest in the automotive industry to increase user involvement early in the design process to create a desirable experience rather than imposed upon users by the system [23]. Regarding the pillar obscuration issue discussed in prior sections, there is a lack of injecting human factors engineering (HFE) attributes early in design. The obscuration and blind spots caused by the pillars continue to cause usability and safety issues in drivers' field-of-view by contributing to fatal and non-fatal accidents, particularly involving pedestrians.

One of the current design practices conducted in automotive involves a human-in-the-loop approach that designers explore users' (e.g., drivers and passengers) comfort, usability, and safety-related attributes via human subjects data collection on early physical mockups. The limitation behind the human-in-the-loop design is often the need to have a wide variety of human subjects to observe their interaction with the system to determine the best solution for the broadest range of users and the effects of design changes. Likewise, engineers can only run a limited number of human subject design experiments due to time, cost, and safety-related restrictions. Within the past decades, computational human modeling research, more commonly referred to as DHM, has gained popularity in product development. DHM uses advanced visualization and analysis modules based on computer-aided engineering (CAE) platforms and includes computational analysis modules such as biomechanics and ergonomics toolkits to predict safety and performance. DHM is widely recognized as an alternate solution to costly and time-consuming human subject data collection activities on physical mockups. The flexibility of running "what-if" scenarios via digital mockups (e.g., CAE models) and creating digital manikins based on anthropometric libraries enable engineers to inject ergonomics early in product development. Although the initial heightened cost of implementing DHM in the design cycle does have a long-term payoff, numerous case studies have shown that designing with DHM improves the overall ergonomics of the final design by reducing the risk of safety and reliability-related concerns [24].

For example, DHM, along with computer-aided design (CAD) technology, has been used to account for pilot's visual fields in the design of jet aircraft cockpits. This approach

has dramatically reduced the need for early physical dummy modeling, prototyping, and human subject data collection, which would result in costly mock-ups. Through DHM and CAD integration, engineers were able to create scenarios to determine what displays were entirely obscured by cockpit components, what displays were visible within different focal ranges, and what areas of the aircraft exterior were visible to the pilot. Overall, making design decisions based on data from target anthropometries and operational requirements before building costly physical prototypes has proved effective in injecting ergonomics into cockpit design [11].

DHM has also been used to account for and analyze large goods vehicle blind spots. This uses volumetric projections to establish the cause and nature of blind spots. This study used six top selling trucks in the UK that have a range of sizes. Additionally, the other design variables that this study considered were the various drivers eye hieghts (driver anthropometry) and mirror designs. This research developede a novel CAD based projection technique which allowed for identification and quantification of key blind spots. This data on the blind spots were then demonstrated to have potential association with scenes that were identified in accident data [25].

2.4 Methodology

This paper introduces an early design digital prototyping approach that integrates DHM and CAD tools to quantify pillar obscuration. Different than prior ergonomics studies that only focused on pillar obscuration with minimal coverage of the actual design parameters, this paper factors numerous variables, including driver and pedestrian anthropometry, type of vehicles, traffic scenes, and different pillar designs, into account.

In this research, two traffic scenes, a crosswalk and turning right, were constructed as CAD models to represent the scenarios taken from the literature where pedestrians are blocked by the A- or D-pillar, respectively. These scenes represent situations that a pedestrian is situated within the pillar obscuration angle; thus, the driver looked but failed to see the pedestrian due to the vision obstruction caused by the pillar. Furthermore, digital replicas (CAD models) of two generic vehicles, a sports car and a sports utility vehicle (SUV), were created based on body-in-white reference models (GrabCad files [1, 2]).

All models created used Solidworks and were stored as Initial Graphics Exchange

Specification (IGES) models to prevent CAD file transfer incompatibilities. These models were imported and positioned into Siemens Jack, the DHM software, to create obscuration simulations with manikin models representing drivers and pedestrians with different anthopometries. Jack's built-in occupant packaging toolkit was used to positioning the drivers via reference points (e.g., pedal and steering wheel). More information about the simulation elements is provided in detail in the following sections. Additionally, a flowchart of the simulation setup, how to run and how to modify simulations for different design variables is provided in Appendix A.

2.4.1 Highway Scene Setup

The highway scenes constructed in this simulation represent some of the most frequently occurring "looked but failed to see" cases that represent typical A- and D-pillar obscurations. These scenes follow highway standards for crosswalks, minor intersections, and bike lanes [14], as shown in figure 2.2.

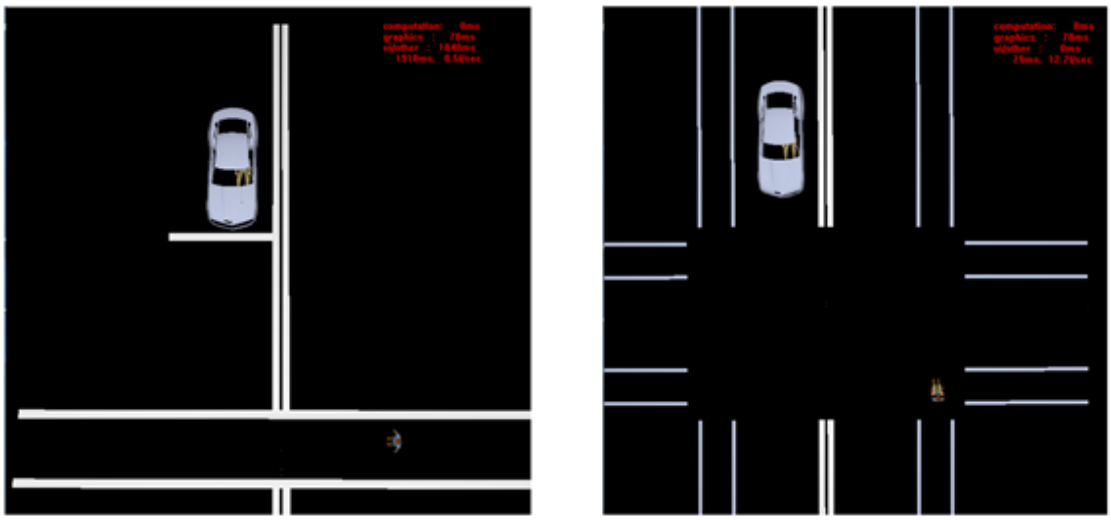

Figure 2.2: Scene Setups for Crosswalk and Intersection with Bike Lanes

The crosswalk scene illustrates a common mishap or accident that happen due to the driver failing to see the pedestrian on the crosswalk. The scene includes a two-lane highway with a crosswalk. The pedestrian is positioned on the forward blind spot, located

diagonal left of the driver's line of sight. In the second traffic scene, a four-lane highway intersection with a bike lane was created. The bicyclist is located within the rear blind spot generated due to the passenger side D-pillar.

2.4.2 Car Models and Pillar Cuts

The two vehicles (a muscle car and an SUV) were chosen intentionally to represent the current trend (thickening pillar) observed in automotive designs. These cars used can be seen in figure 2.3 below.

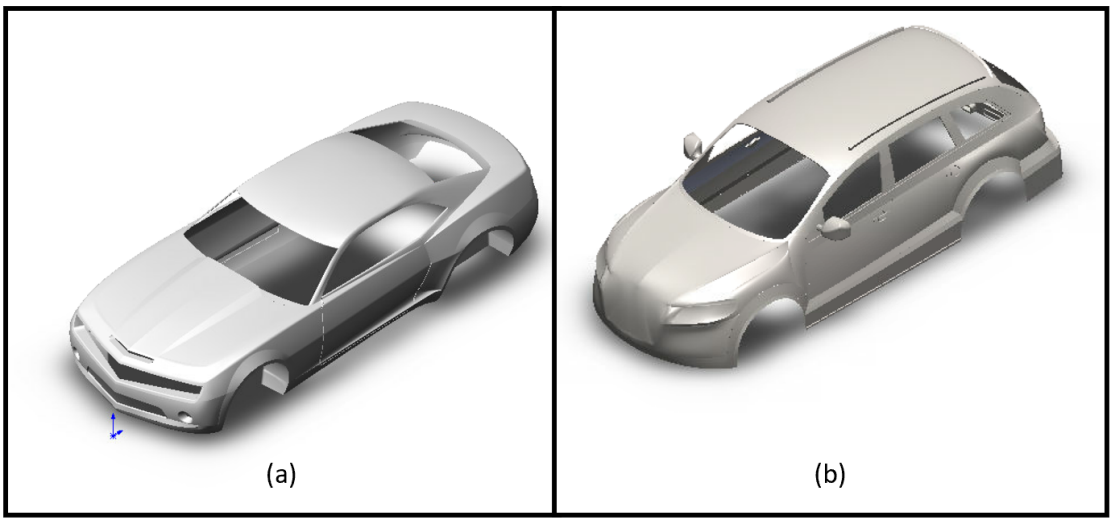

Figure 2.3: (a) Sports Car, (b) SUV

Thicker, rollover, and aerodynamics friendly pillar designs represented in these generic vehicle models cause larger front (A-pillar) and rear (D-pillar) blind spots. In addition to the traditional (opaque - no cut) pillars found in regular vehicles, the simulation environment also included three see-through pillar designs with different geometric cuts: ellipse cut, triangle cut, and honeycomb cut (See figure 2.4). The geometric cuts represent structural elements typically used in buildings, bridges, and other static structures. These cuts focus on material removal from the traditional pillars while sustaining comparable structural integrity. For example, honeycomb is known to provide sufficient strength in natural and human-made structures. The form factor is widely used to lighten structures,

particularly in automotive and aviation domains. Furthermore, to keep the data analysis consistent, the area removal is standardized. The geometric cuts made in each pillar have the same surface area removed, approximately 172 cm^2.

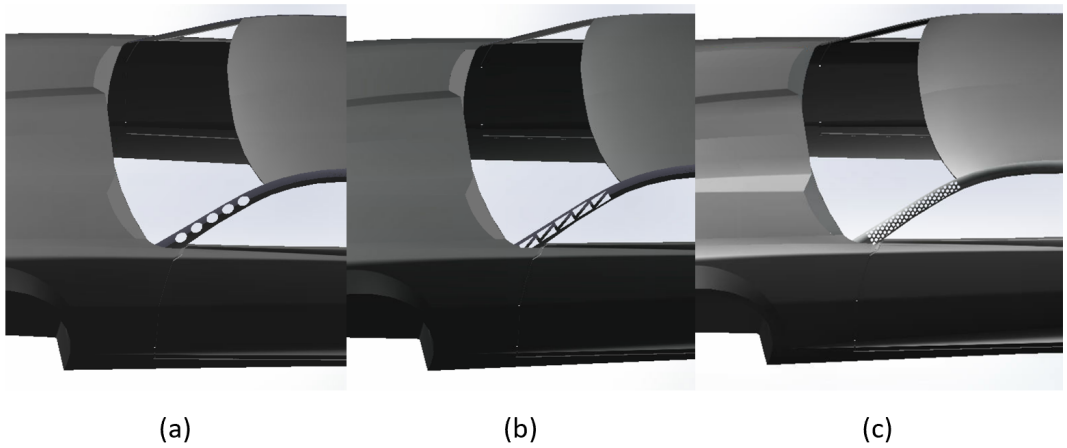

Figure 2.4: (a)A-pillar Ellipse Cut, (b)A-pillar Triangle Cut, (c)A-pillar Honeycomb Cut

2.4.3 Manikin Anthropometry

The study includes six computational manikins created via the Anthropometric Survey of U.S. Army Personnel (ANSUR) anthropometric database. The simulation environment includes 5^{th}, 50^{th}, and 95^{th} percentile male and female drivers to reproduce a broader coverage of drivers. Each manikin was positioned in both vehicles (muscle car and SUV) using Siemens Jack software's prebuilt occupant packaging tools, which use occupant packaging blueprints with specific reference points [1, 2]. This toolkit enables us to assign a fixed standard driving posture to each DHM manikin. Therefore, it eliminates the need to adjust body joints manually and reduces the possibility of having incorrect driving postures.

Furthermore, four different pedestrian anthropometries based on the ANSUR database were used in the scene setup to represent pedestrians. In addition to 5^{th} percentile female, 50^{th} male, and 95^{th} percentile male, a 12-year-old male child model was used in this study to represent an even smaller target that is highly likely to be obscured by pillars

Table 2.1: Pedestrian Heights

Pedestrian Anthropometry	Standing Height (cm)	Bike Height (cm)
Child	158	166
5th Female	161	168
50th Male	181	197
95th Male	196	207

during road crossing and intersections. Table 2.1 presents standing and on bike heights associated with pedestrian anthropometries.

2.4.4 Coverage Zone Analysis

After CAD models were imported into Jack software and manikins were created, the next step was to set scene simulations to quantify percent obscuration. The simulation model included scene, car, pillar cut, and anthropometry combination in Jack. Table 2.2 shows a tabulated version of these variables. This table shows the simulation variables used. Listing each categorical variable as xmn, where x1n = Scenes, x2n = Cars, x3n = Cuts, x4n = Driver Anthropometry and x5n = Pedestrian Anthropometry. This table shows all variables used which all possible combinations were used in this study. A total of 384 scenes were simulated. To quantify obscuration percent loss, Coverage Zone Analysis was used. The toolkit addresses what percent of a target plane is not obscured by objects in the way from the point of reference. To run this analysis, the Coverage Zone Analysis needs four inputs; target plane, point of reference, horizontal and vertical resolution. The analysis outputs the percent visible and a visual representation, based on how much of the opaque surfaces (imported CAD models) obscure the manikins' peripheral vision.

For this study there are a lot of steps which are needed to setup the coverage zone analysis. As discussed above the coverage zone analysis need four inputs in order to output the percent area obscured. These inputs can be seen in figure 2.5 below. To create the target plane you must open the coverage zone analysis window and then select create target plane. Then to dimension the plane you have to create rulers that measure the height and width you desire because the target plane does not have a way to make it the exact dimensions you need. Then once the target plane has dimensions it needs it is positioned where the pedestrian is positioned. Following this the eye point needs to

Table 2.2: Variables Used in Case Study

Scene (x1n)	Car (x2n)	Cut (x3n)	Driver Anthro. (x4n)	Pedestrian Anthro. (x5n)
Two Lane	Muscle Car	no cut	5th Male	Child
			50th Male	
		Ellipse cut	95th Male	5th Female
		Triangle cut	5th Female	50th male
Turning Right	SUV		50th Female	
		Honey comb cut	95th Female	95th male

be selected which is done by going into the object hierarchy and selecting the manikin and segments. There is no selecting the actual eyes within JACK so one has to select a part of the head that it would project from. For this study the back of the head was used because of trails done with other segments. Finally, the resolution needs to be setup which requires a horizontal and vertical resolution. Unfortunately, this resolution does not work the way one would expect instead the max resolution is can have is the dimensions of the target plane. Therefore, the resolution dimensions match that of the target plane used in the simulation. Additionally, "Ignore Human Geometry and Highlight Obstruction Segments" need to be selected to ensure the simulation outputs the percent area obstructed correctly. This Coverage Zone Analysis setup requires a lot of additional setups in order to run and proved to be more problematic to setup correctly. The output of the percent area visible was recorded and tabulated in excel for future analysis.

2.4.5 Structural Analysis

Finally, a simplified FEA study of the pillar model was performed based on the FMVSS 216 roof crash test standards. The reaction forces and displacements associated with the static loading condition were evaluated to check whether pillar models with see-through geometric cuts meet roof-crush test requirements. FMVSS 216 roof crash test standards

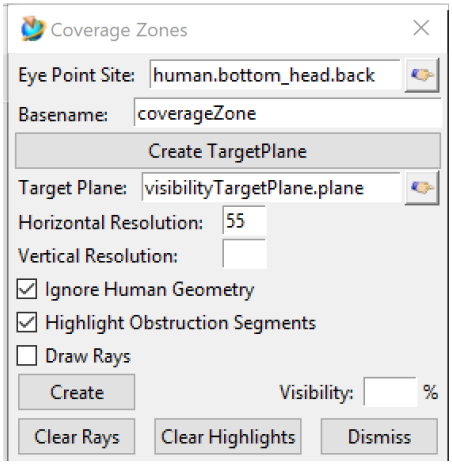

Figure 2.5: Coverage Zone Analysis Window

state that a vehicle must withstand a load of 1.5 times the unloaded vehicle's weight. Although the FEA study was not the focus of the proof of concept study presented in this paper, further data regarding structural integrity provided additional information about the pillar models' performance from the percent obscuration and structural integrity perspective. sssdsd For this study, the muscle car model was used due to the lack of D pillar as compared to the SUV model; thus, it would experience a more significant static loading. The FEA study follows assumptions based on previous research and tests done on pillar strength analysis [26, 27]. Furthermore, high-strength alloy steel was used based on research articles addressing A-pillar structure design [28]. This simplified FEA was performed in Solidworks.

The total force applied on a single A-pillar was assumed to be approximately around one-fourth of the vehicle's total weight, which is about 1672 kg; thus, the roof crash test load applied normal to the pillar upper tip was equal to 4.2 kN. The Von Mises stress was then calculated and compared to the yield strength. Additionally, the displacement was calculated and compared to the standards and no cut model.

2.5 Results and Discussion

This section contains the results of the case study that was done with the proposed methodology. This is to provide validation for the methods used and to see how different

pillar cuts perform in a small case study. The results include the results of the coverage zone analysis done for both the Sport Car's and the SUV's A and D pillar. This analysis output percent area visible of the target plane (the pedestrian) which has been tabulated and plotted for observation, further analysis, and discussion. Following these general descriptive statistics of the results us provided with a discussion to give a deeper understanding of the tabulated data. Finally, to ensure the pillars in the case study meet the FMVSS roof crash test standards.

2.5.1 Coverage Zone Analysis

The coverage zone analysis is analysis that analyzes how much of target plane is visible. This will then out put a percentage based on eye point, resolution, and target plane geometry. To determine the target plane, the pedestrian's anthropometry was used with a five percent increase on the height and the width is kept at a width of 55cm. This five percent increase is used to account for a range of anthropometries. The Coverage Zone Analysis was done for all possible combination of the variables, see in the Methodology section. Each output of percent area visible was then recorded for future analysis.

To help with understanding of the coverage zone analysis and what the output looks like, figure 2.6 shows the a snapshot of what the result of the coverage zone analysis look like for the SUV at the crosswalk scene.This coverage analyses shown in the figures were done for the 50th percentile driver and pedestrian anthropometry and shows the crosswalk scene for the SUV. The coverage zone analysis output shows the percent area visible and highlights the parts which are obstructed with red and the visible parts with green. For the example, the honeycomb cut had the largest increase compared to the Triangle cuts

Once the Coverage Zone Analysis was done and collected for all possible scene combinations for these two cars. The data was plotted on histograms to better understand the data and the trends. The histograms for the sport car's scenes can be seen in figures 2.7 and 2.8 and the SUV's can be seen in figures 2.9 and 2.10 below.

These plots show the percent visible on the x-axis and a count of results that were near that percentage on the y-axis. These histograms show that the trend for each group for all cars and scenes seem to be similar with certain spikes in the percent area visible and some reflecting normal trend and others with a log-normal. Overall, the graphs show

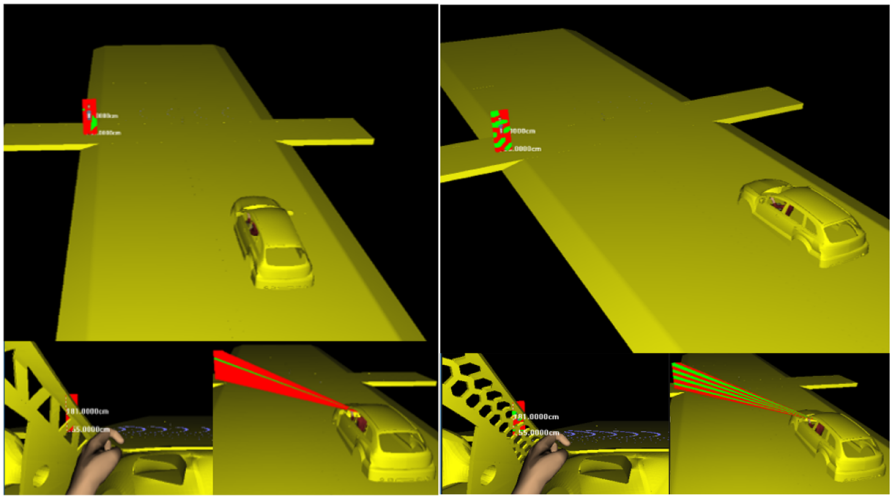

Figure 2.6: SUV Coverage Zone Analysis Results for Crosswalk Scene 50th Percentile Male Driver and 50th Percentile Male Pedestrian

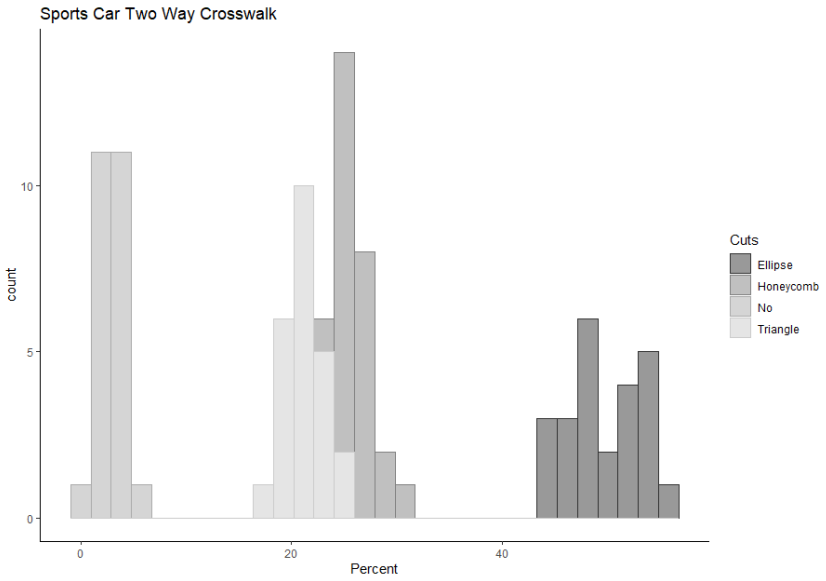

Figure 2.7: Histogram for Sports Car Crosswalk scene (A-pillar)

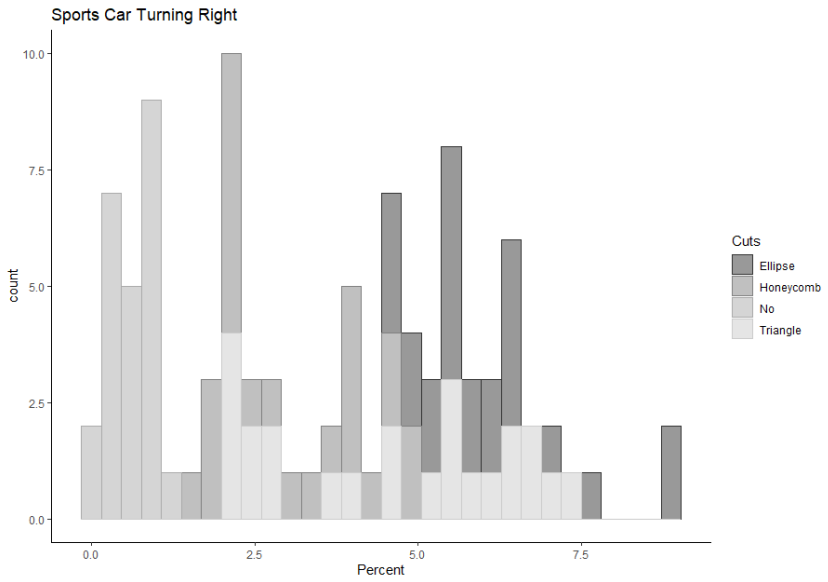

Figure 2.8: Histogram for Sports Car Turning Right Scene (D-pillar)

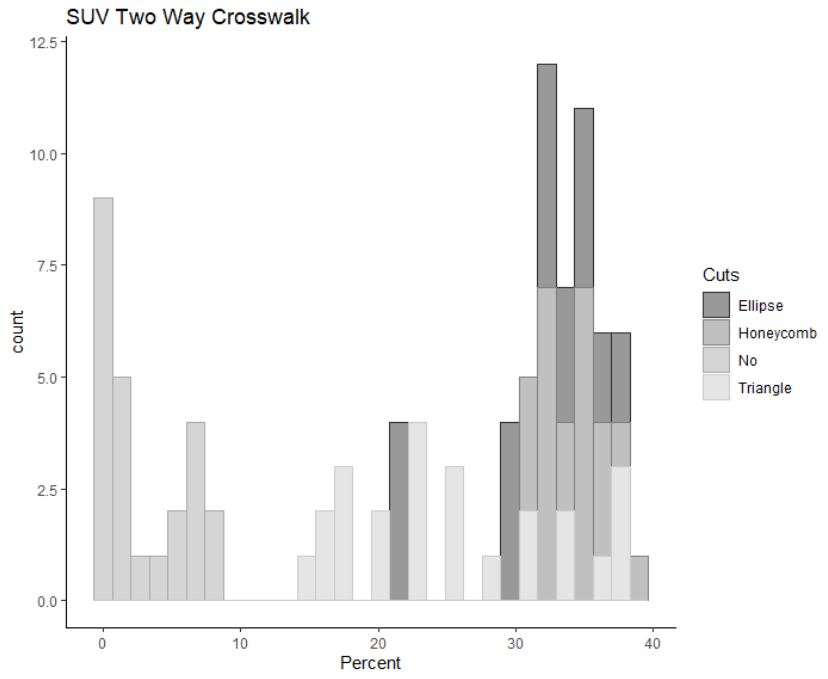

Figure 2.9: Histogram for SUV Crosswalk Scene (A-pillar)

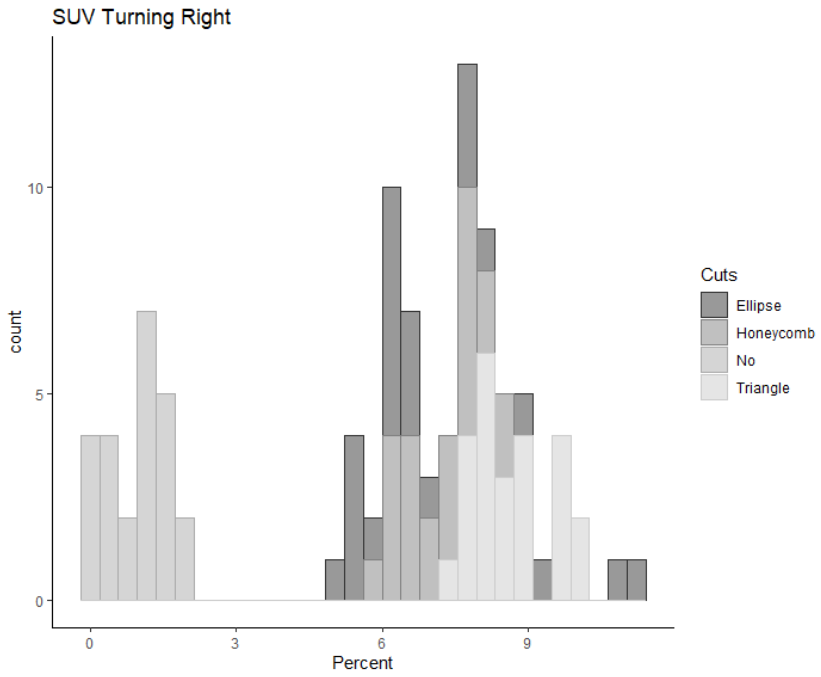

Figure 2.10: Histogram for SUV Turning Right Scene (D-pillar)

that percent area visible is improved when provide cuts in the pillars. However, the main thing to take away from these plots are the differences between the A pillar scenes (two lane highway crosswalk) and the D pillar scenes (turning right). They show that the cuts made in the A pillar, although having the same area removed for each cut, have different results based on the geometry. Where the D pillar shows similar results between all cut geometries. This helps understand that the A pillar is more significantly affected by the cuts made in the pillars, which is also reflected in the percent area visible with the A pillar having higher overall percentages.

After creating histograms for a visual analysis and understanding a brief statistical analysis using general statistics table was done for further understanding. Below in table 2.3 and 2.4 mean, variance, and standard deviation of the entire case study has been tabulated. These results show an overall increase in percent area visibility for the cuts made in the pillars compared to the traditional, no cut, pillar. Additionally, Coverage Zone Analysis results for the A pillar show the largest overall increase in visibility for the ellipse pillar cut for the sports car with an overall mean of 49.49% and the honeycomb pillar cut for the SUV with an overall mean of 34.05%. The lowest increase in visibility was the triangular cut for both the sports car with an overall mean of 21.28% and the SUV with an overall mean of 24.48%. Coverage Zone Analysis results for the D-pillar show the largest overall increase in visibility for the ellipse pillar cut for the sports car with an overall all mean of 5.92% and the triangle pillar cut for the SUV with an overall mean of 8.60%. The least increase in visibility was the honeycomb pillar cut for both vehicles with an overall mean of 2.89% for the sports car and 7.19% for the SUV. Although it may seem like the honeycomb performed the worst for visibility it had the least variance, with 2.26 for the A-pillar in the sports car and 4.24 for the A-pillar in the SUV.

The plotted and tabulated results show that the cuts made in the SUV for both the A and D pillar that the holes provided similar vision improvements. Where for the sports car's A and D pillar there is one that clearly performed the best. This can especially be seen in the plots created for the ellipse cut for the sports car Two Lane Crosswalk scene. When comparing the results of the A to D pillars the A-pillar had a larger percent area visibly than the D-pillar, due to the driver manikin being positioned closer to the cut made in the pillar, allowing for a larger range of vision. Although the cuts performed differently compared to each other, the results were definitive that cuts made in pillars improve visibility. However, some cuts performed better or worse depending on the driver

Table 2.3: Mean, Variance and Standard Deviation for Sports Car

Sports Car		Mean	Variance	Standard Deviation
No Cut	A-Pillar	2.56	1.54	1.81
	D-Pillar	0.50	0.10	0.31
Ellipse Cut	A-Pillar	49.48	12.84	3.66
	D-Pillar	5.92	1.32	1.17
Triangle Cut	A-Pillar	21.28	3.42	1.89
	D-Pillar	4.16	3.41	1.85
Honeycomb Cut	A-Pillar	26.30	2.26	1.54
	D-Pillar	2.89	1.22	1.13

Table 2.4: Mean, Variance and Standard Deviation for SUV

SUV		Mean	Variance	Standard Deviation
No Cut	A-Pillar	1.49	8.33	0.82
	D-Pillar	0.66	0.33	0.57
Ellipse Cut	A-Pillar	30.95	25.77	5.19
	D-Pillar	6.87	2.74	1.69
Triangle Cut	A-Pillar	24.48	54.11	7.51
	D-Pillar	8.60	0.69	0.83
Honeycomb Cut	A-Pillar	34.06	4.24	2.10
	D-Pillar	7.19	0.54	0.75

and pedestrian anthropometry.

2.5.2 Structural Analysis

The results from the structural analysis show that all pillars meet the minimum requirement of a deflection, which can be seen in figures 2.11 and table 2.5. However, since this is a simplified A-pillar a test the pillars will be compared to the A-pillar without cuts. The pillars with the ellipse cuts performed the best with a max deflection of 0.3227 mm and a Von Mises stress of 23.87 Mpa. Where the Honeycomb performed the worst with a max deflection of 0.9578 mm and max stress of 93.8 Mpa. These results were not expected. The pillars with the triangle and honeycomb cuts were anticipated to perform the best based on their structural uses within buildings and within nature (trusses and beehives). Although the results were not expected, all pillar designs did not exceed the 127mm displacement meetings the FMVSS 216 standards.

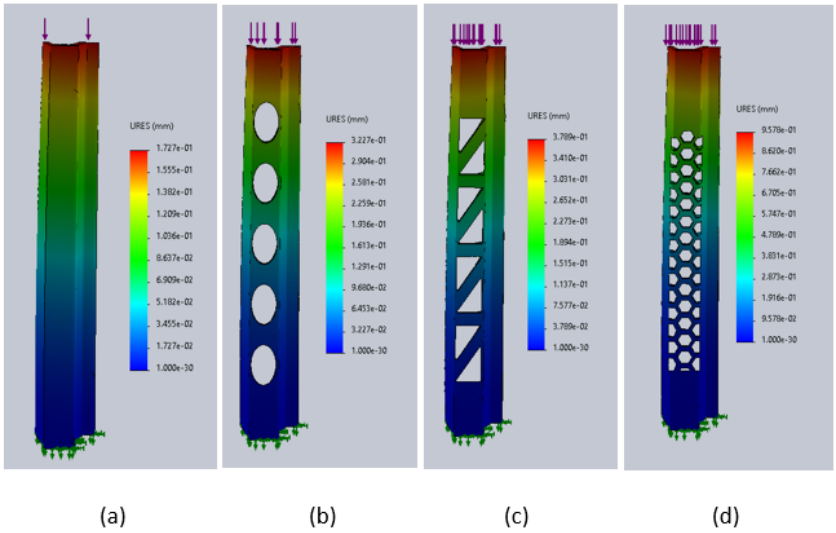

Figure 2.11: Visuals of Deflection from FEA

Based on the results, hole cuts on car pillars can provide a means to help alleviate obscuration that traditional car pillars cause. Although different cuts performed better than others when looking at driver anthropometry, ellipse cuts performed the best overall. Ellipse cuts provided the best visibility for the A-pillar, consistent results for the D-pillar

Table 2.5: Max Stress and Deflection of A-Pillar

FEA Results	Cut Type			
	No Cut	**Ellipse Cut**	**Triangle Cut**	**Honeycomb Cut**
Max Stress (Mpa)	9.057	23.87	65.84	93.8
Deformation (mm)	0.1727	0.3227	0.3789	0.9578

and provided the greatest structural integrity with the lowest max deformation and lowest max Von Mises stress. However, the honeycomb cut provided the most consistent results for the coverage zone analysis. Therefore, it would be worth examining different setups for the honeycomb cuts, like size of hexagon, how many hexagons and their orientations.

2.6 Conclusion and Future Work

This proof of concept has shown to be a successful implementation of using Digital Human Modeling (DHM) to analyze and improve car pillar design.The case study used in this proof of concept used a combination of different variables to create different scenes found in literature. The variables included; scene, car type, pillar type, cut type and driver and pedestrian anthropometry. The highway created and imported into Jack was either a crosswalk (which is associated with the A-pillar simulations) or a turning right (which is associated with the D-pillar simulations). The vehicles imported and positioned into the Jack scene were either the muscle car or the SUV. The manikins were generated in Jack for the driver and the pedestrian and positioned based on occupant packaging or literature. Setting up for the Coverage Zone Analysis involved creating a target plane which was generated based on the pedestrian's anthropometry and position, selecting an eye point and resolution. Once an eye point, target plane and resolution are defined, These results were then recorded and analyzed. Additionally, a simplified structural analysis was done to make sure the pillar cuts met the necessary standards.

The results showed that cuts made in the A and D pillar help alleviate the vision obstruction. However, A-pillar cuts had a much larger impact on improving vision than the cuts made in the D-pillar. The cuts that performed the best depended on the car and the scene, but the ellipse cut seemed to perform best overall and the honeycomb cut performed the worst but outputted the most consistent. A similar result was seen with the structural analysis using the FEA where the ellipse pillar cut was the most

structurally sound and honeycomb pillar cut was the least.

This research and methodology has a number of limitations. This research requires a lot of manual manipulation of the variables which can have lots of human error associated with it. Automation could fix this problem and possible allow for more simulations to be run with a varity of different variables, but JACK does not allow for any easy way to automate vision analysis. Additionally, the positioning of manikins in the simulation were done using standards found in literature or done based on the researchers intuition. However, most drivers do not have the same driving setup which makes standardizing posture and position a large assumption and requires some sort of physical prototyping. Furthermore, providing cuts in a car pillar may seem to be a good design in theory but requires further testing and analysis because pillar design and manufacturing is far more complex and may cause some design limitations. There are a number of other limiations within this research and methodology but this provides a basis for future researchers to work off of which may lead to improved car pillar design.

The next phase in this research is to increase the number of computational simulations done through increasing the number of scenes, cars and anthropometries used.Currently, work is being done on increasing the coverage zone data set to include a total of four scenes and four vehicles.This data set can then be used to increase understanding and potentially surrogate models to have predictive models that allow for interpolation of the results. Since currently this simulation cannot be automated this predictive model could allow for a means to understand untested variables (e.g. anthropometries in between tested one and different cut sizes). Additionally, this research could use the coverage zone data collected and higher fidelity structural analysis of the A-pillar to do multi-objective optimization to look at the best pillar design possible. These scenes could also be used in virtual or augmented reality (VR or AR) to test human subjects rather than virtual manikins.Data collected from the coverage zone analysis, surrogate model, optimization model or all could be used to compare computational methods to VR and/or AR to create a better understanding of how accurate the computational methods are. This research has a lot of potential and could be taken many directions.

Chapter 3: Obscuration Analysis of Car Pillar Designs using Digital Human Modeling: Design of Experiments

3.1 Abstract

Many drivers who are involved in accidents involving pedestrians and cyclists have fallen victim to the looked but failed to see due to a vision obstruction caused by the pillars- vertical posts that connect the car bodies to the roof. There have been many solutions proposed in literature to solve this issue, from conventional ways of moving the pillar and thinning the pillar to even suggesting the use of cameras or augmented reality. These solutions prove to be expensive due to the changes needed in the vehicle design and the physical prototyping required to test these solutions. Additionally, some of these solutions have been found not to eliminate the obstruction caused by pillar geometry. This paper works off a previous proof of concept that proposes a methodology based on digital human modeling (DHM) research that explores A- and D-pillar vision obstructions to mitigate the need for human subject testing and physical prototyping. The previous proof of concept paper does a small case study which looks at different car pillar designs comparing the traditional car pillar to three other car pillar designs with geometric cuts for a sports car and SUV. This paper provides a more in depth look at this methodology using a Design of Experiments (DoE) which provides a deeper understanding to the methods used. This DoE uses a coverage zone analysis to quantify obscuration of a combination of four cars, four different traffic scenes, four pillar designs with geometric cuts, six driver anthropometries and four pedestrian anthropometries. The coverage zone data is collected as percent area visible data and is analyzed using a non-parametric variance analysis and a pairwise comparison using the Kruskal Wallis test and Wilcoxon Rank Sum comparison. Overall, the objective of this research is to (1) to perform and evaluate coverage zone analyses to assess the percent area visible of a pedestrian, (2) computationally compare and evaluate the performance of traditional car pillars and those with geometric cuts in terms of improvement in blind spots caused by A-pillars and D-pillars and (3) provide statistical proof that car with see-through pillars perform

better than traditional car pillars in terms of vision obstruction. The results of this DoE and research show that there is overwhelming evidence that car pillars with geometric cuts made (see-through pillars) improve visibility of blind spots caused by traditional car pillars.

3.2 Introduction

The focus of this paper is to better understand how visibility while driving can be improved by creating cuts in car pillars. This is done by creating a Design of Experiment (DoE) of different cars in different scenarios with other independent variables to see how visibility changes with a combination of these variables. This experimentation is purely computational and focuses on using Digital Human Modeling (DHM), Siemen's Jack, to evaluate the different cars and pillar designs. Data is then collected for each possible combination of the independent variables to understand the response. This data for each car and scene was collected and analyzed using a non-parametric variance analysis, Kruskal-Wallis, to analyze the cuts made to the original pillars. Once these analyses were completed, they were tabulated and a Post Hoc test was done for the Kruskal-Wallis. These analyses are to increase the understanding of how cuts within car pillars may improve the driver's visiblity. They will then be examined to see if they meet the null or alternative hypotheses of the analyses. Since the Kruskal-Wallis tests compares medians of k groups, the null hypothesis is the medians of the group are equal and the alternative is that they are not equal.

3.3 Literature Review and Background

This section is to provide a background about the need for this research and experimentation. It provides an understanding of why the scenes used were chosen, why the A and C/D pillar are being focused on and how digital human modeling (DHM) can used to run experiments to understand human interaction and visibility. As well as why the statistical models were used. Finally, a summary of what state of the art methods are being used to try to solve the vision obstruction caused by the car pillars

3.3.1 Car Pillar Vision Obstruction

Within vehicle design there is a strong need for car pillars to be reevaluated to improve visibility. Literature suggests car design used to focus on engine performance, design, and structure [13, 29]. However, more modern vehicle design has focused on comfort and safety of the passengers. Visibility falls into both categories with higher visibility making the driver and passengers better understand and prepare for the environment around them. A large portion of environmental information is gathered through by human eye, up to 90% in most cases [15, 30]. This makes it increasing important to consider visibility in early vehicle design. One of the largest limiting factors in vision for car design are the car pillars seen in figure 3.1 [31]. These pillars provide structure support and the number of pillars and their geometry vary depending on the car; like having large pillars or steep pillar angles [1, 2, 31]. Although these pillars are a crucial element of the car design, they cause blind spots which limit the vision of the driver making it make it more difficult to see and detect pedestrians while. Making it necessary to reevaluate how these pillars are designed and implemented.

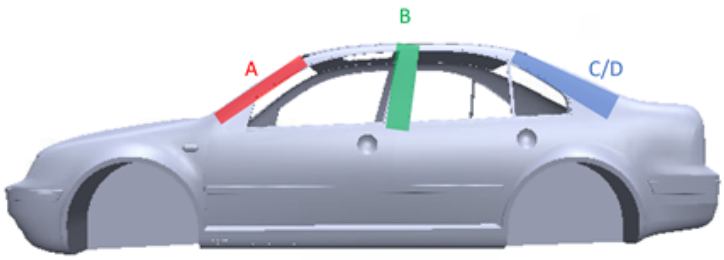

Figure 3.1: Labeled Car Pillars[]

3.3.2 Traffic Scenes and Cars

Vision obstructions caused by car pillars is a crucial element in this research. However, it is also important to know in what traffic situations these car pillars cause the most vision obstruction. Literature suggests through various case studies that pedestrians on foot, pedestrians on a bicycle and changing lanes are the most impacted by these vision

obstructions [29]. These accidents heavily relate to yielding crosswalks and turning left or right at an intersection (A-pillar for turning left and C/D pillar for turning left) [31]. Mainly, these accidents are due to a "looked but failed to see" affect where the driver looked in the direction of the pedestrian but either failed to register the pedestrian or the pedestrian was obscured [15, 31].

Since all cars have varying geometry and different pillar positions and types, it is important to understand what kinds of cars have been addressed and related to poor vision. According to a 1996-2003 database the main kind of cars to be involved in pillar related accidents were two door sedans, SUV and pickup trucks [32]. Additionally, four door cars tend to have larger pillars due to there being less pillars and can cause a decent amount of vision obstruction, however they were not considered in the database. Furthermore, the study these researchers conducted found that most lane change and intersection crashes related to the A and C/D pillar obstructions [32].

3.3.3 Current Solutions

Although it may not seem the vision obstruction caused by car pillars has not been addressed, it is not a novel topic of research. The understanding of the vision obstruction caused by the A-pillar is well documented and researched. Additionally, there has been several solutions that have been proposed to address the issue. These solutions include but are not limited to:

- Slimming A-pillar to improve driver's field of vision [29]
- Changing location to change influence of A-pillar on driver visibility [31]
- Detection systems that use cameras to show the driver what is behind or next to the pillar [33]
- Transparent car pillars [34]

These solutions provide a way to solve the issue of the vision obscuration caused by car pillars. The slim A-pillar provides a smaller obscuration angle than the traditional A-pillar, some vehicle designs have begun to implement this slim designs [29]. However, there is a concern for the structural integrity it provides and for there not being room to add additional safety features such as air bags [33]. As for the changing the location of the pillar itself, it is a quick solution that helps increase the driver's vision by providing a wider range of vision but does not altogether take care of the issue of the pillar causing a vision

obscuration [31]. Finally, the idea of using detection systems and creating transparent car pillars seems to be a sufficient method of eliminating the vision obstruction caused by the car pillars. However, as the research suggests, the use of cameras and/or augmented reality is a costly solution and as for the transparent pillar case, has a long way to go before this could become close to being commercially available [34].

3.3.4 Digital Human Modeling for Vison Analysis and Experimentation

DHM has been a growing tool withing early design stages and is continuing to grow. For instance, within industrial engineering DHM has continued to be a reliable tool to predict and assess how human interaction will play out [24, 25]. In many cases DHM is used to see how different postures while running and maintaining operations affect the person performing the task [12]. Allowing for a deeper understanding of the human and machine relationship. Additionally, DHM has been begun to be used in vision assessment relating to vehicle design. In fact, in one paper addresses using DHM to assess how well a driver can see using mirror and trying to look past the A-pillar [35]. This not only confirms that A-pillars cause an obscuration to vision but also provides evidence that DHM vision assessment is a very useful tool to address and analysis the site of a driver [20, 35]. Additionally, it is mentioned that researchers and vehicle manufactures should provide a more in-depth study of how vision is affected by A-pillars in different scenarios and should find ways to improve or minimize the size of the A-pillar. Providing further need for this DoE and for deeper understanding of how car pillars affect driver vision and assess ways to help solve this problem.

3.4 Methodology

This paper uses a DoE to setup, run and analyze car pillar design in various cars, scenes and with varying driver and pedestrian anthropometries. This set up includes several assumptions for the DoE and the Analysis. It assumes cars are stopped, drivers stay in the same posture and positions, pedestrians remain in the same position for each scene setup and this is a static not a dynamic simulation. The setup for these experiments will be laid out along with the specifics of how the variables were created and setup.

The setup for the DoE uses four cars, four cuts, four scenes, six driver anthropometries and four pedestrian anthropometries. A total of 1,536 were created and analyzed. A flowchart explaining the experiment's hierarchy of branches can be seen in figure 3.2 below. This flow chart breaks each step into different categories for each variable. Each of these categories are further explained in the follow sections to show how they were setup and why they were chosen. All these variables are considered independent variables.

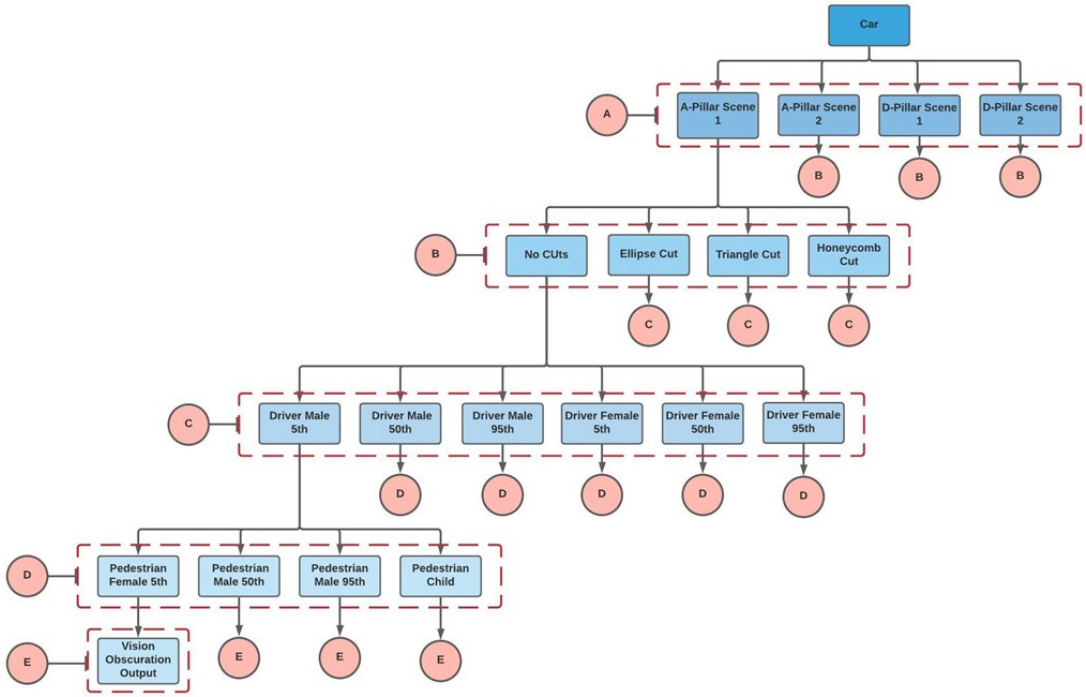

Figure 3.2: Diagram of DoE Setup

3.4.1 Variable Setup

These next subsections describe how each independent variable was setup. These various setups were used in combination to create the scene for each simulation.

Setup 1: Car Model The first part to be setup was the car models. A total of four car models were chosen: a sports car, sedan, SUV, and a pickup truck. These models were created using SolidWorks surface modeling which were based on the blueprints of

the vehicles chosen. Additionally, models found on Grabcad were used to help increase the accuracy of these models [1–4]. An image of these car models can be seen below in figure 3.3. .

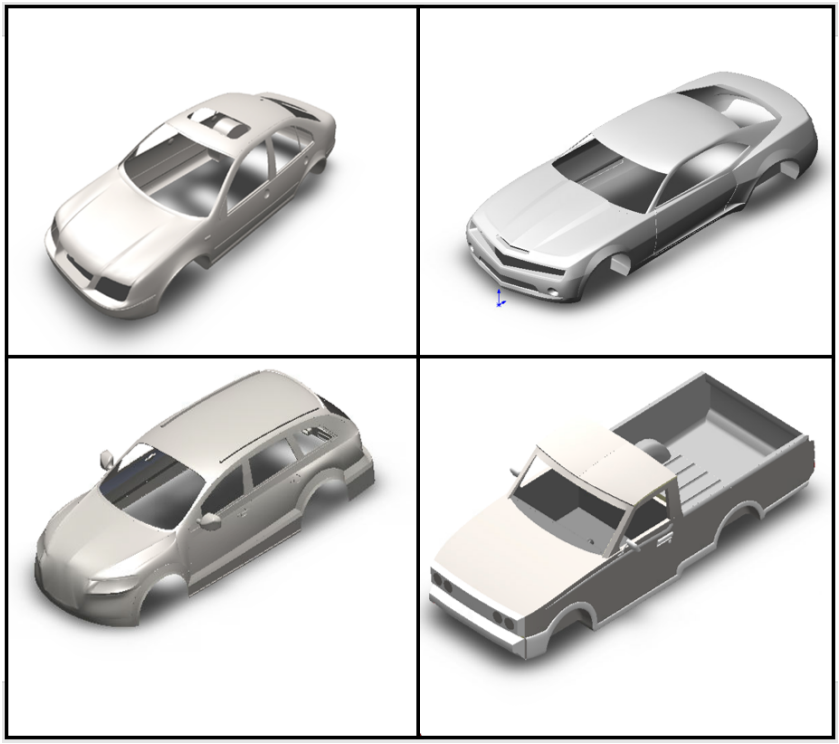

Figure 3.3: Car Models Used

Setup 2: Cuts The second part to be setup was the cuts on each of the car models. There are a total of four cuts on each cars A and C/D pillar. These cuts consist of none, ellipse, triangle, and honeycomb cut. Each of these cuts consist of the same total area removed, 172 cm$\hat{2}$. These cuts were cut based the designers' preferences for placement and form factor. Meaning that the size, count, and position of these cuts are assumed to differ but only the geometry of the cut will be focused on for this experimental setup. The kinds of cuts can be seen below in figure 3.4.

Setup 3: Scenes The third part to be setup were the scenes. These scenes chosen were the ones seen in literature which can be seen in the literature review above in the Literature Review section. The scenes chosen are split into scenes focusing on the

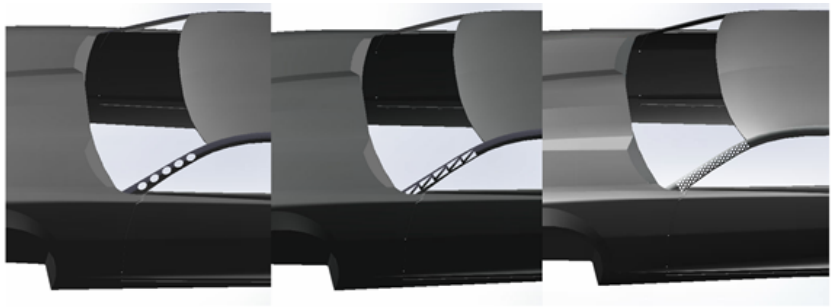

Figure 3.4: Car Pillars Cuts used: Ellipse, Triangle and Honeycomb

A-pillar and scenes focusing on the C/D-pillar. The scenes chosen for the A-pillar were a four-way intersection with the vehicle turning left with an oncoming biker being blocked by the A-pillar and a vehicle driving on a two-lane intersection with a pedestrian crossing the street and being blocked by the A-pillar. The scenes chosen for the D-pillar were a four-way intersection with a car turning right and a pedestrian coming up from behind on a bike and a car attempting to parallel park with a pedestrian standing the parking spot. These scenes were based on highway standard for intersections, crosswalks, bike lanes and highways (reference). Depictions of these scenes can be seen below in figure 3.5.

Setup 4: Driver Anthropometry A total of six driver anthropometry were used. Trying to get a wide range of anthropometries the 5th, 50th and 95th percentile male and female from the ANSUR database were used. These drivers were then positioned according to occupant packaging of the vehicle used. The manikins were first setup by using a tool in the occupant packaging toolkit called Posture Prediction. The Posture Prediction uses predefined posture based on dimensions of stored vehicle information. The postures chosen were the closest relating to the that of the vehicle being used in the scene. The car used in the scene setup and the posture prediction used can be seen below in table 3.1. Once posture prediction was used the manikins were placed according to the vehicle standards.

Setup 5: Pedestrian Anthropometry With these being manual simulations and the simulation count increasing it was decided that four pedestrian anthropometries would be used. It was decided the smallest, median, and tallest driver anthropometries would be used; 5th percentile Female and 50th and 95th percentile male, respectively.

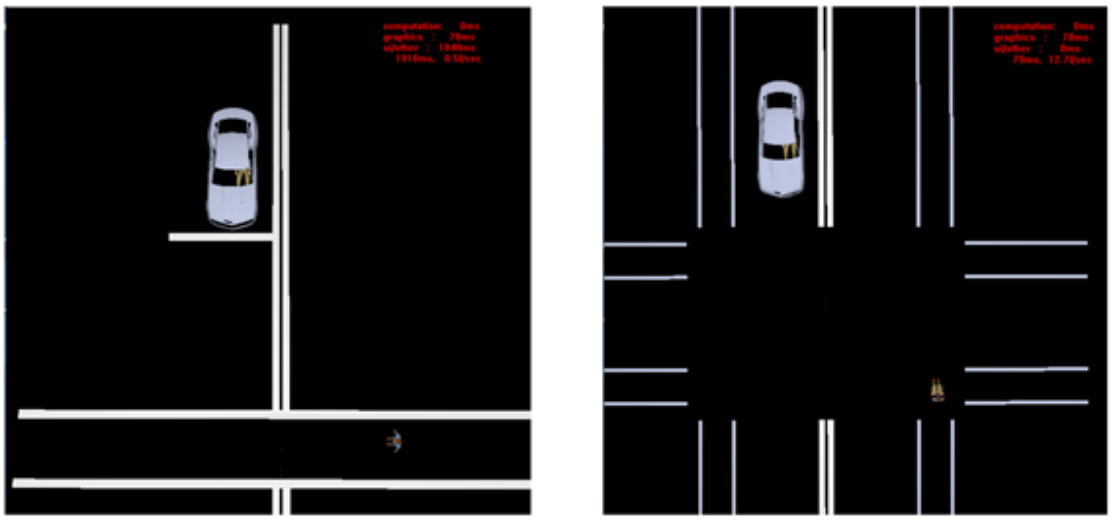

Figure 3.5: Traffic Scenes Used: Left - Crosswalk Two lane Highway, Right - Intersection with Bike Lane

Table 3.1: Posture Prediction for Each Car

Vehicle Type	Car Model Used	Posture Prediction – Existing Vehicle
Sedan	Volkswagen Jetta	Toyota Camry
Sports Car	Chevy Camaro	Chevy Camaro
SUV	Audi Q7	Jeep Grand Cherokee
Pickup Truck	Toyota Hilux	Ram Pickup

For the fourth anthropometry a 12-year-old male child was used because children are some of the most difficult to see for drivers.

3.4.2 Coverage Zone Analysis

Once the independent variables were setup a coverage zone analysis was done for each possible combination, creating the dependent variable. A coverage zone analysis assesses the percent area visible of a target plane (user defined) visible from a target from an eye point site and how much the target plane is being obscured by an object. This analysis requires additional setup beyond the dependent variables, requiring setup of the target plane, defining the eye point, and defining resolution for the analysis. It is important to note that this analysis uses a static 2D plane, so it does not consider the dynamics or 3D geometry of the real world but allows for a snapshot moment of the scene. The window display for the coverage plane analysis can be seen in figure 3.6 below.

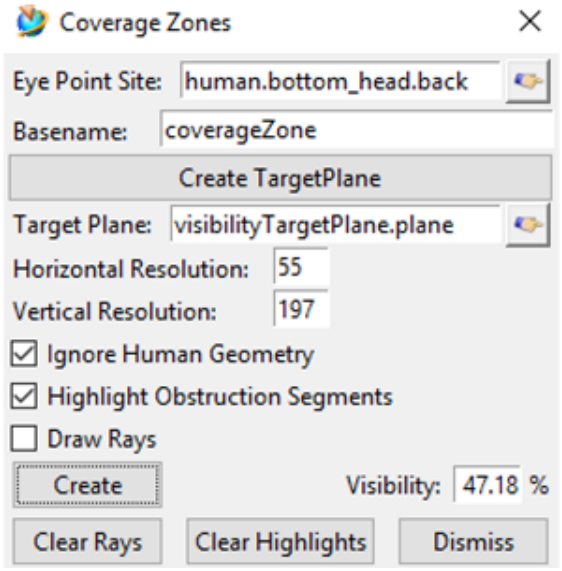

Figure 3.6: Coverage Zone Analysis Window with Example of 95% Male Driver and 50% Male Biker

Target Plane Setup: First, was setting up the coverage plane which was based on anthropometry of the driver. This means a total of eight coverage planes need to

Table 3.2: Target Plane Dimensions

Anthropometry of Pedestrian	Standing Target Plane Dimensions	Biker Target Plane Dimensions
Child	55 cm x 158 cm	55 cm x 165 cm
5th Percentile Female	55 cm x 162 cm	55 cm x 168 cm
50th Percentile Male	55 cm x 181 cm	55 cm x 197 cm
95th Percentile Male	55 cm x 196 cm	55 cm x 207 cm

be setup because there are a total of four pedestrian anthropometries but two scenes the pedestrian is standing and in the other two the pedestrian is riding a bike. Then to account for changes between anthropometry and variability between anthropometry movement, the coverage plane was made 5% taller than the pedestrians height on and off a bike. Additionally, a standard width of 55cm was used for all coverage zones. A table containing the target plane dimensions can be seen in table 3.2.

Eye Point Setup: Setting up the eye point required selecting a point on the driver manikin to project from. Different segments of the manikin can be seen in the object hierarchy, seen in figure 3.7 below. It was found the best segment to select for this eye point was the back of the head of the driver manikin.

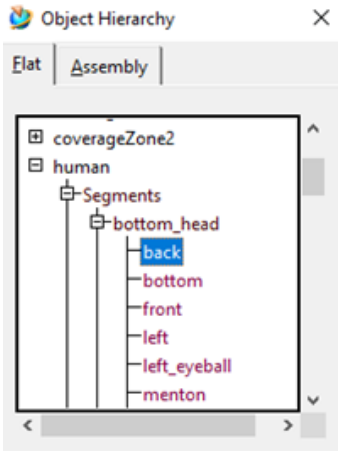

Figure 3.7: Object Hierarchy Window

Resolution Setup: The final aspect to setup for this analysis was the resolution which needs a vertical and horizontal resolution. For this experiment it was desired

to have the highest resolution possible without drastically affecting the output. Some testing was done to see what the best possible resolution was. It was discovered that the resolution does not do what was expected. Instead, the largest resolution could be without compromising the shape of the target plane was 1cm x 1cm. This means the resolution max used in the analysis was the dimensions of the target plane, horizontal resolution: 55 and vertical resolution: the height of the target plan used.

3.4.3 Statistical Analysis

With all independent variables and coverage zone setup the analysis could be run. The results of the analysis give a percent area of the coverage plane. The values of each coverage zone analysis were then stored on an excel table which separates each car, cut and scene. These tabulated data was then reformatted to get ready to be analyzed and compared. This data was setup in such a way that each car was analyzed based on scene, cut, driver anthropometry and pedestrian anthropometry.

Using the tabulated data set a statistical analysis was done to better understand the data collected, to allow for direct comparison, to look at significance and to help draw statistical conclusions. These focus on looking how the cuts compared to the original pillars and how the cuts performed compared to each other but also ask questions of how different anthropometries affect overall visibility.

To address the data, set categorical variables needed. Categorical variables are variables which assign each unit observation to a particular group or nominal category based on a qualitative property. Therefore, variables like cut type, driver anthropometry and pedestrian anthropometry can be used in variance analyses. With the categorical variables setup and organized, analyses could begin. The first thing that needed to be addressed was how the cuts performed compared to the original pillars. It is assumed that the No Cut will have a drastically different variance than of the cuts made so a non-parametric method to compare the distribution and significance. The method chosen was the Kruskal–Wallis which does not assume a normal distribution of the residuals. Once a statistical analysis of the cut type compared to the original pillar was done, the original pillar was removed from the dataset to allow for a comparison between cut types. This cut comparison was done using Wilcoxon Rank Sum Post Hoc pairwise comparison.

3.5 Results

With the DoE being completed and the data compiled it could now be addressed and analyzed. This data will be assessed based on observations, plots, and statistical analyses. Whether cuts improved vision compared to the standard pillar, what pillar performed the best for each car and scene and what driver anthropometry was impacted the most by the pillar changes will all be addressed throughout this section.

3.5.1 DoE: Coverage Zone Analysis

The initial result of this experiment was the output of the coverage zone analysis itself. Below in figure 3.8 there are four coverage zone analyses along with driver field of vision for original pillar and the three different pillar cuts.

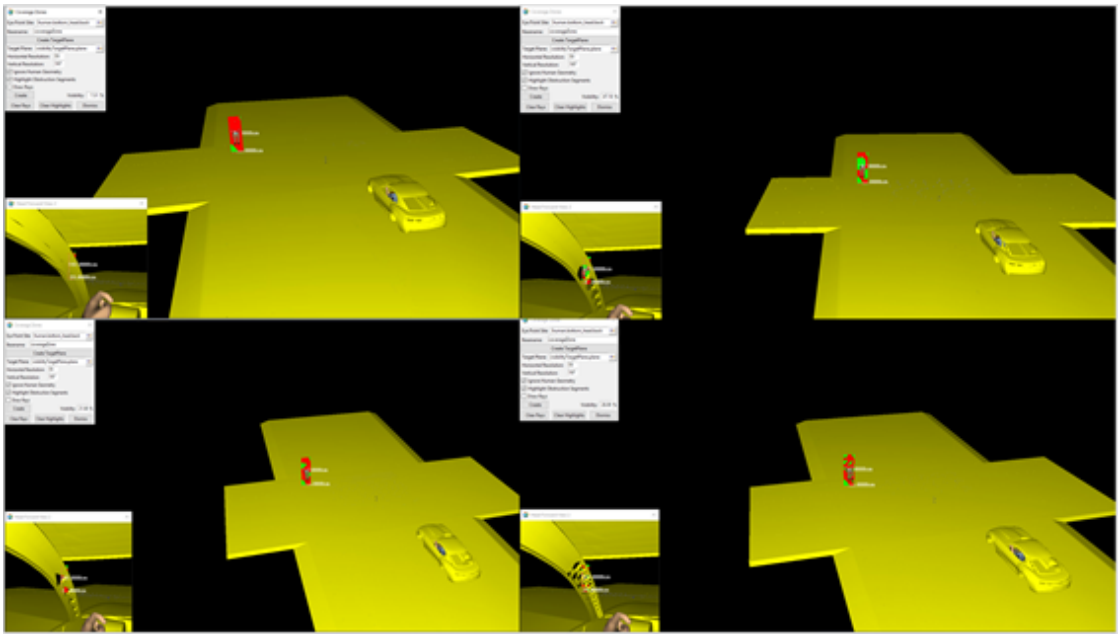

Figure 3.8: Coverage Zone Analysis Examples for the Crosswalk A-pillar Scene for Each Cut and the 95th Percentile Driver and 50th Percentile Pedestrian

Although the cuts themselves changed, all the other independent variables were kept the same for the simulations in the figure; Camaro, turning left scene, 95th percentile male driver and 50th percentile male pedestrian. When looking at the figure the pillar

with the ellipse cut performed the best for this scene and car. However, the results tend to vary depending on the scene and car used along with different combinations of the other independent variables.

All possible combinations along with the percent area visible results and standardized results have been tabulated. After looking at the fully tabulated data set it can be assumed the driver's vision is increasing as cuts are made in the pillars. It can also be noted, through observation of the tabulated data, that the A-pillars vision is more significantly affected by the cuts made in the pillar.

3.5.2 DoE: Plots of Scenes

After addressing the initial observations made of the data, histograms were created for each scene and the cuts. These histograms were created for all pillar types (including the original pillar). Plots for each car and scene can be seen in Appendix A. These show the count of the percent area visible of the target planes for each scene and car. This it to provide a visual representation of how the cuts made in the pillar improve the overall vision of the drivers.

Looking at the observed data it can be noted that all the cuts seem to improve the visibility of the driver. Additionally, it can be noted that the cuts increased the visibility more for the A-pillar scenes compared to the C/D pillar scenes. After collecting and plotting the data a deeper understanding is needed. Therefore, there is a need for a statistical analysis. This also allows for the hypotheses to be addressed.

3.5.3 DoE: Statistical Analysis

Following the initial observations and initial plots created a statistical analysis was run to better understand the data set and to allow for statistical conclusions to be drawn. Before the statistical analysis can be drawn a further understanding of the data set is needed. To do this, box plots were created for each of the vehicles and the scenes. Then normality and variance were addressed based on initial observations made of the box plots. Plots for the muscle car, SUV, sedan, and pickup truck can be seen in Appendix A.

When addressing the data plotted on the box plots the variance is drastically different

for the A-pillar no cut and the rest of the cuts. Additionally, most of the data did not follow a normal distribution. This means a non-parametric variance analysis is needed so it does not need to rely on normal data and allows for different variances. With this understanding, Kruskal-Wallis Analysis was chosen to compare the dataset to each other mainly focusing on the comparison between cuts and the standard pillar.

3.5.4 Kruskal-Wallis Analysis

The Kruskal-Wallis test is a non-parametric variance analysis or comparison which is used to determine if the medians of two or more groups. This helps provide evidence the cuts made in car pillars improve visibility. For this kind of comparison there are four sets of assumptions that must be checked. These assumptions are as follows:

Assumption 1: Dependent variable should be measured at the ordinal or continuous level.

Assumption 2: Independent variable should consist of two or more categorical independent groups.

Assumption 3: Each observation should be independent.

Assumption 4: Each group has same or similar shape. This means the same variability.

Assumptions 1 through 3 are easily observed and should be followed as the experiment is being setup and conducted. As for the 4th assumption, the distributions must be compared. Additionally, this assumption does not need to be met in order to run the Kruskal-Wallis variance analysis, this just determines if conclusion are drawn about medians if met or means if not met. This has already been done above in the histograms and box plots seen in the Appendix. After comparing the distributions of the plots above, it can be concluded that the plots do not meet assumption 4.

The next step of the Kruskal-Wallis variance analysis was to state the hypotheses to know what is to be expected from the test conducted. The hypotheses can be seen below. For this dataset, the null hypothesis states the mean of the no cut percent area visibility is equal to the mean of the percent area visibility of each cut. Where the alternative hypothesis states the mean of the no cut percent area visibility is not equal to the mean of the percent area visible of each cut. The null hypothesis was examined for each car and scene. Based on initial observations of the data and plots created it can be assumed

that the data will confirm the alternative hypotheses rather than the null hypotheses. Additionally, following the Kruskal-Wallis test a pairwise comparison using the Wilcoxon Rank Sum test with a continuity correction was done for a better understanding of the significance of how the cuts differed from each other and how each to the original pillar of the car.

H0: $\text{mean}_{(}nocutpercent) = mean_{(}cutpercent)$

HA: rejected

Appendix A has tables which provide a summary of the statistics for each car showing the results for each scene and cut. Providing the population size, mean, standard deviation, median and interquartile range (IQR).

The Kruskal-Wallis test run for each car can be seen below in table 3.3, which contains all scenes for the vehicle. Below each table is a discussion of the tables to help with understanding of the analysis.

For all cars and all scenes there is overwhelming evidence that the percent visibility changed when adding cuts in the pillars compared to not having cuts in the pillars, with an average p-value of 1.85e-13 for the Sports car, 8.77e-13 for the SUV, 1.61e-13 for the Sedan and 2.20e-16 for the Pickup. This supports the alternative hypothesis that the means are not equal.

3.5.5 Pairwise Comparison: Wilcoxon Rank Sum

To further understand how all the cuts compared in this experiment the results of the Wilcoxon Rank Sum test for each car and can be seen in tables 3.4, 3.5, 3.6 and 3.7 . Additionally, below each table is a discussion of the results to create a better understanding.

Any values which are lower than 0.05 provide evidence that the two pillar cuts being compared are statistically different. Based on the tables above all pillar cuts for all cars have overwhelming evidence that the mean percent area visibility is different from the pillars with no cuts. Based on the values of percent area visibility being close to zero for the no cut pillar this implies the pillars that do have cuts will provide better visibility. Then further analysis of the results shows how each cut type compare to each other for each car and scene. All different pillar cuts showed overwhelming or strong statistical difference between cuts, except for the Honeycomb cut for the parallel parking scene

Table 3.3: Kruskal Wallis Results for Each Car and Scene

Sedan- Kruskal-Wallis				**Sports Car - Kruskal-Wallis**			
Scene	**Chi-Squared**	**df**	**p-value**	**Scene**	**Chi-Squared**	**df**	**p-value**
Turning Left	59.532	3	7.40E-13	Turning Left	59.532	3	7.40E-13
Two Lane Highway	61.439	3	2.90E-13	Two Lane Highway	88.35	3	2.20E-16
Turning Right	61.439	3	2.90E-13	Turning Right	88.35	3	2.20E-16
Parallel Parking	61.439	3	2.90E-13	Parallel Parking	88.35	3	2.20E-16
SUV - Kruskal-Wallis				**Pickup - Kruskal-Wallis**			
Scene	**Chi-Squared**	**df**	**p-value**	**Scene**	**Chi-Squared**	**df**	**p-value**
Turning Left	60.725	3	4.11E-13	Turning Left	87.806	3	2.20E-16
Two Lane Highway	61.878	3	2.33E-13	Two Lane Highway	87.487	3	2.20E-16
Turning Right	87.487	3	2.33E-13	Turning Right	87.487	3	2.20E-16
Parallel Parking	87.487	3	<2.2e-16	Parallel Parking	87.487	3	2.20E-16

Table 3.4: Sports Car Wilcoxon Rank Sum Pairwise Comparison

Sports Car - Wilcoxon Rank Sum Test				
Scene	**Cuts**	No	Ellipse	Triangle
Turning Left	Ellipse	3.70E-09	-	-
	Triangle	3.70E-09	3.70E-09	-
	Honeycomb	3.70E-09	3.70E-13	5.00E-09
Two Lane Highway	**Cuts**	No	Ellipse	Triangle
	Ellipse	3.70E-09	-	-
	Triangle	3.70E-09	3.70E-13	-
	Honeycomb	3.70E-09	3.70E-09	1.30E-08
Turning Right	**Cuts**	No	Ellipse	Triangle
	Ellipse	6.00E-09	-	-
	Triangle	6.00E-09	0.0227	-
	Honeycomb	6.00E-09	1.50E-08	0.0033
Parallel Parking	**Cuts**	No	Ellipse	Triangle
	Ellipse	6.10E-09	-	-
	Triangle	6.10E-09	0.07	-
	Honeycomb	6.10E-09	0.757	0.051

Table 3.5: SUV Wilcoxon Rank Sum Pairwise Comparison

SUV - Wilcoxon Rank Sum Test				
Scene	**Cuts**	No	Ellipse	Triangle
Turning Left	Ellipse	6.10E-09	-	-
	Triangle	6.10E-09	2.07E-02	-
	Honeycomb	6.10E-09	4.64E-01	2.80E-04
Two Lane Highway	**Cuts**	No	Ellipse	Triangle
	Ellipse	6.10E-09	-	-
	Triangle	6.10E-09	1.05E-01	-
	Honeycomb	6.10E-09	1.52E-01	2.10E-04
Turning Right	**Cuts**	No	Ellipse	Triangle
	Ellipse	6.10E-09	-	-
	Triangle	6.10E-09	1.30E-04	-
	Honeycomb	6.10E-09	1.80E-01	2.30E-06
Parallel Parking	**Cuts**	No	Ellipse	Triangle
	Ellipse	6.10E-09	-	-
	Triangle	6.10E-09	0.07	-
	Honeycomb	6.10E-09	0.757	0.051

Table 3.6: Sedan Wilcoxon Rank Sum Pairwise Comparison

Sedan - Wilcoxon Rank Sum Test				
Scene	**Cuts**	No	Ellipse	Triangle
Turning Left	Ellipse	4.90E-09	-	-
	Triangle	4.90E-09	2.38E-03	-
	Honeycomb	4.90E-09	1.40E-03	5.79E-02
Two Lane Highway	**Cuts**	No	Ellipse	Triangle
	Ellipse	3.50E-09	-	-
	Triangle	3.50E-09	1.58E-01	-
	Honeycomb	3.50E-09	1.80E-04	3.74E-02
Turning Right	**Cuts**	No	Ellipse	Triangle
	Ellipse	5.90E-07	-	-
	Triangle	1.90E-06	7.90E-01	-
	Honeycomb	9.40E-06	7.90E-01	9.00E-01
Parallel Parking	**Cuts**	No	Ellipse	Triangle
	Ellipse	8.50E-05	-	-
	Triangle	1.10E-05	0.194	-
	Honeycomb	4.70E-06	0.014	0.194

Table 3.7: Pickup Wilcoxon Rank Sum Pairwise Comparison

Pickup - Wilcoxon Rank Sum Test				
Scene	**Cuts**	No	Ellipse	Triangle
Turning Left	Ellipse	6.60E-10	-	-
	Triangle	6.60E-10	1.80E-08	-
	Honeycomb	6.60E-10	8.70E-08	4.60E-09
Two Lane Highway	**Cuts**	No	Ellipse	Triangle
	Ellipse	9.00E-10	-	-
	Triangle	9.00E-10	3.90E-08	-
	Honeycomb	9.00E-10	5.50E-08	4.60E-09
Turning Right	**Cuts**	No	Ellipse	Triangle
	Ellipse	3.50E-10	-	-
	Triangle	3.50E-10	3.70E-13	-
	Honeycomb	3.50E-10	7.80E-01	3.70E-09
Parallel Parking	**Cuts**	No	Ellipse	Triangle
	Ellipse	6.10E-09	-	-
	Triangle	6.10E-09	0.0459	-
	Honeycomb	6.10E-09	0.9753	0.0078

which has no statistical difference. For the SUV for the cuts that had no statistical difference were the ellipse compared to the honeycomb for the Turning left scene, the honeycomb and triangle cut for the Two-Lane Highway scene, the ellipse compared to the Honeycomb for the Turning Right scene and all cuts for parallel parking scene. For the Sedan, the pillar cuts that had not statistical difference were the ellipse cut compared to the triangle cut for the Two-Lane Highway scene, all cuts for the Turning Right scene and all cuts for the Parallel parking scene. Finally, for the pickup truck the cuts that had not statistical difference were the ellipse cut and honeycomb cut for the Turning Right scene and the ellipse cut and honeycomb cut for the Parallel Parking Scene.

The results of these statistical analyses run show that there is overwhelming evidence that cuts made in car pillars improve mean percent area of visibility, proved by the comparisons having a p-value of less than 0.05. Additionally, the cuts made in the pillars that had the same area removed but different geometric shaped seemed to perform better for some cars. Based on the results this seems to relate mostly with the A-pillar. This is probably due to the A-pillar being so close to the driver, so differences are easily seen when the cuts are changed. As for the D-pillar it is further away from the driver and may be hard to tell the difference and in some cars the D-pillar is set more vertical making cuts with the same area have similar results.

3.6 Conclusion

With a great deal of research providing evidence that car pillars are a leading cause of "looked but failed to see" accidents, research regarding how to understand and improve visibility is ever more prevalent. Additionally, providing a way to understand the pillars visibility problems and how modifications would affect the visibility is even more crucial. This allows for the for money to be saved and time to be saved later down the engineering design process during the prototyping phase. The research not only shows how to setup a design of experiments using different cars, traffic scenes, pillar types and cuts, different driver anthropometry and pedestrian anthropometry, but also provides with the use of statistical testing and analyses provides evidence that visibility can be improved using cuts made in the car's pillars. The tests which were done were the Kruskal-Wallis test and the Willcoxon Rank Sum for a post hoc pairwise comparison. The Kruskal-Wallis test provided overwhelming evidence that adding a cut to a pillar changes the mean percent

area visibility for the driver and that since the no cut experiments ran had approximately zero visibility, it provides evidence the cuts improved visibility. This supported the alternative hypothesis that the mean values of the groups were not the same. While the Wilcoxon Rank Sum test provided evidence that some cuts made for different cars and scenes, although having the same area removed, differ in percent visibility output. This pairwise comparison highlights some of the limitations with research and provides a need for future work to be continue this research.

This research has created a need for pillar designs that include cuts to be examined. Additionally, this research provides evidence that assessing pillar design and visibility is possible in early stages of the design process with the help of CAD and DHM models and simulations. Making alternative methods to pillar vision obstruction needing to be re-evaluated because methods such as cameras or sensors, although effective, are costly and require physical prototyping. There are a lot of directions this research can go but it is important to understand the limitations first. Although this research provided evidence that pillar visibility can be improved using cuts made in the pillars, it does not provided evidence to what the best cut design is. This research only took into consideration four cars, four scenes and most importantly four pillar designs with different geometries but the same area removed. This research/ experiment did not examine different size pillar cuts, various cut locations and tapering of the cut. Furthermore, full pillar designs were not examined. Only thickened versions of the Body in White structures were used which means not including the assemblies and pieces like air bags, covers and wiring. Also, another limitation includes the driver and pedestrian positioning being determined my researcher. These are not all the contributions and limitations but just a few of the major ones.

This DOE is just the beginning of this research and is just trying to lay the foundation for future researchers to work off. First off, this research should be done with more dependent and independent variables to increase the significance of the findings. Example, size and shape of the cuts should be varied, more anthropometries should be use, different angles and tappers of the cuts and more scenes and cars would be of value as well. Additionally, this DOE should now be setup in a virtual reality and/or augmented reality lab to compare the data collected using DHM to allow for a better understanding of the accuracy of using DHM for visibility of car pillars. This research would pair well with the use of optimization techniques as well. It would be worth re-running this experiment with

the increased variables and the variable area removed and using some sort of surrogate modeling to create a predictive model about the untested setups. Another way this could be paired with optimization techniques is by using something like topology optimization to have material optimally removed from the pillar to ensure the pillar meets safety standards. Then this pillar design could be tested against the geometric pillar designs already tested to see how they compare. There are many paths and directions this research could go. This experiment and the results should be used by future researchers to further this field of study.

Chapter 4: Conclusions

The purpose of this research was to quantify vision obstruction of car pillars and was to provide a method to assess car pillar design improvements using DHM analysis and to observe the significance effects on these design parameters on visibility using CAD and Jack DHM simulation. The proof of concept allowed for observations on how car pillars performed in various scenarios and how cuts made in the pillars improve visibility. Then to further observe and provide preliminary statistical proof that vison obscuration is improved by making cuts in car pillars a DoE was conducted. Which showed that any form of cuts improves percent visibility based which was proved using the Kruskal Wallis test and pairwise comparison of each pillar design using the Wilcoxon Rank Sum test. Although this DoE provided statistically accurate results the statistical significance and deeper understanding would be improved using physical experiments using human-subject testing. Additionally, this research would further benefit for the use of automation process which would allow for highly accurate and repeatable experiments. This would allow for a higher fidelity experimentation, more experiments, and setups to be conducted and for a larger data set which would allow for better and more accurate conclusions to be drawn.

This methodology and results would greatly benefit if it was to be continued by pairing automation, optimization, and physical experimentation. For example, if processes like CAD/ solidworks models (vehicles and scene environments), Coverage zone analyses and statistical analyses were to be automated then they could be shared and easily repeated for duplications of the experimentation or for future experiments. If optimization techniques were used for both pillar design and for the results of automated experiments, then optimized pillar structures which meet the roof crash FMVSS standards and provide the least visibility could be extrapolated. However, this may create another challenge of manufacturability. Finally, with physical prototypes either virtual or augmented reality would allow for a better testing of these car pillar designs and give a proof of how well the computational methods perform for testing these designs. This research and thesis provide a good start for how to evaluate different car pillars vision obstruction and

provides a way to evaluate these designs computationally. Furthermore this research through computational methods proved creating cuts in preexisting car pillar designs can minimize vison obstruction and help decrease looked but failed to see accidents.

Bibliography

[1] A Chauhan, *Free cad designs, files 3d models: the grabcad community library.*

[2] MH Masum, *Free cad designs, files amp; 3d models: the grabcad community library.*

[3] O Najera, *Free cad designs, files amp; 3d models: the grabcad community library.*

[4] HM Mehedi, *Free cad designs, files amp; 3d models: the grabcad community library.*

[5] B Pipkorn, J Lundström, and M Ericsson, "Improved car occupant safety by expandable a-pillars", International journal of crashworthiness **17**, 11–18 (2012).

[6] N Filion, *Thicker, rollover-friendly a-pillars make for massive blind spots*, Nov. 2019.

[7] S Turner, L Sandt, J Toole, R Benz, and R Patten, "Federal highway administration university course on bicycle and pedestrian transportation. publication no. fhwa-hrt-05-133.", US Department of Transportation (2006).

[8] R Noe, *Eighth grader successfully makes a car's a-pillars invisible, using standard technology*, Nov. 2019.

[9] Y He, "Research on the possibility of camouflaged a-pillars by using the quadrangular prism of self invisibility", American Journal of Vehicle Design **4**, 1–10 (2018).

[10] CL Su, CJ Lee, MS Li, and KP Chen, "3d avm system for automotive applications", in 2015 10th international conference on information, communications and signal processing (icics) (IEEE, 2015), pp. 1–5.

[11] X Zhang and DB Chaffin, "Digital human modeling for computer-aided ergonomics", Handbook of Occupational Ergonomics. Taylor & Francis, CRC Press, London, Boca Raton, 1–20 (2005).

[12] D Lämkull, L Hanson, and R Örtengren, "A comparative study of digital human modelling simulation results and their outcomes in reality: a case study within manual assembly of automobiles", International Journal of Industrial Ergonomics **39**, 428–441 (2009).

[13] M Carlier, *Ford: ramp;d spending*, Feb. 2020.

[14] K Rumar, "The basic driver error: late detection", Ergonomics **33**, 1281–1290 (1990).

[15] R Moore and HR Smith, "Paper 6: visibility from the driver's seat: the conspicuousness of vehicles, lights and signals", in Proceedings of the institution of mechanical engineers, conference proceedings, Vol. 181, 4 (SAGE Publications Sage UK: London, England, 1966), pp. 56–70.

[16] EM Szumska and PT Grabski, "An analysis of the impact of the driver's height on their visual field range", in 2018 xi international science-technical conference automotive safety (IEEE, 2018), pp. 1–6.

[17] F Vargas-Martin and MA Garcia-Perez, "Visual fields at the wheel", Optometry and Vision Science **82**, 675–681 (2005).

[18] B Peacock and W Karwowski, *Visual aspects in vehicle design, automotive ergonomics* (Taylor & Francis London, 1993).

[19] M Sivak, B Schoettle, M Reed, and M Flannagan, "Body-pillar vision obstructions and lane-change crashes", Accident reconstruction journal **19**, 56–58 (2009).

[20] C Quigley, S Cook, and R Tait, "Field of vision (a-pillar geometry)-a review of the needs of drivers: final report.", (2001).

[21] M Reed, *Intersection kinematics: a pilot study of driver turning behavior with application to pedestrian obscuration by a-pillars*, tech. rep. (University of Michigan, Ann Arbor, Transportation Research Institute, 2008).

[22] B Pipkorn, J Lundström, and M Ericsson, "Safety and vision improvements by expandable a-pillars", in 22nd international technical conference on the enhanced safety of vehicles (esv) national highway traffic safety administration, 11-0105 (2011).

[23] NHTS Administration et al., *Federal motor vehicle safety standards; roof crush resistance; phase-in reporting requirements*, 2010.

[24] X Sun, R Houssin, J Renaud, and M Gardoni, "A review of methodologies for integrating human factors and ergonomics in engineering design", International Journal of Production Research **57**, 4961–4976 (2019).

[25] S Summerskill, R Marshall, S Cook, J Lenard, and J Richardson, "The use of volumetric projections in digital human modelling software for the identification of large goods vehicle blind spots", Applied ergonomics **53**, 267–280 (2016).

[26] A LANZOTTI, A VANACORE, and C PERCUOCO, "Robust ergonomic optimization of car packaging in virtual environment", in *Advances on mechanics, design engineering and manufacturing* (Springer, 2017), pp. 1177–1186.

[27] N Saba, J Rishmany, I Tawk, and M Daaboul, "Optimization of the production process of an a-pillar using a differential thickness profile approach via fea", (2017).

[28] KS Naik and A Patil, "Structural analysis and optimization of biw a-pillar used in automobiles", International Journal for Advance Research and Development **3**, 91–96 (2018).

[29] Y Cho and B Han, "Application of slim a-pillar to improve driver's field of vision", International Journal of Automotive Technology **11**, 517–524 (2010).

[30] S Ahn, Y Jeon, J Yun, P Kang, J Ko, and P Park, "Development of a forward visibility assessment tool based on visibility angle", International Journal of Automotive Technology **16**, 1051–1055 (2015).

[31] AC Santos, A Gerez, A Pádua, P Genaro, R Silva, and S Ferreira, *The influence of a-pillar obscuration/location on driver visibility*, tech. rep. (2020).

[32] M Sivak, B Schoettle, MP Reed, and MJ Flannagan, "Body-pillar vision obstructions and lane-change crashes", Journal of safety research **38**, 557–561 (2007).

[33] P Beresnev, A Tumasov, D Zeziulin, D Porubov, and L Orlov, "Development of a detection road users system in vehicle a-pillar blind spots", in Iop conference series: materials science and engineering, Vol. 386, 1 (IOP Publishing, 2018), p. 012008.

[34] YL Chang, YM Tsai, and LG Chen, "A real-time augmented view synthesis system for transparent car pillars", in 2008 15th ieee international conference on image processing (IEEE, 2008), pp. 1972–1975.

[35] R Marshall, S Summerskill, and S Cook, "The use of dhm based volumetric view assessments in the evaluation of car a-pillar obscuration", Advances in Applied Human Modeling and Simulation **255** (2012).

APPENDICES

Appendix A: Appendix A

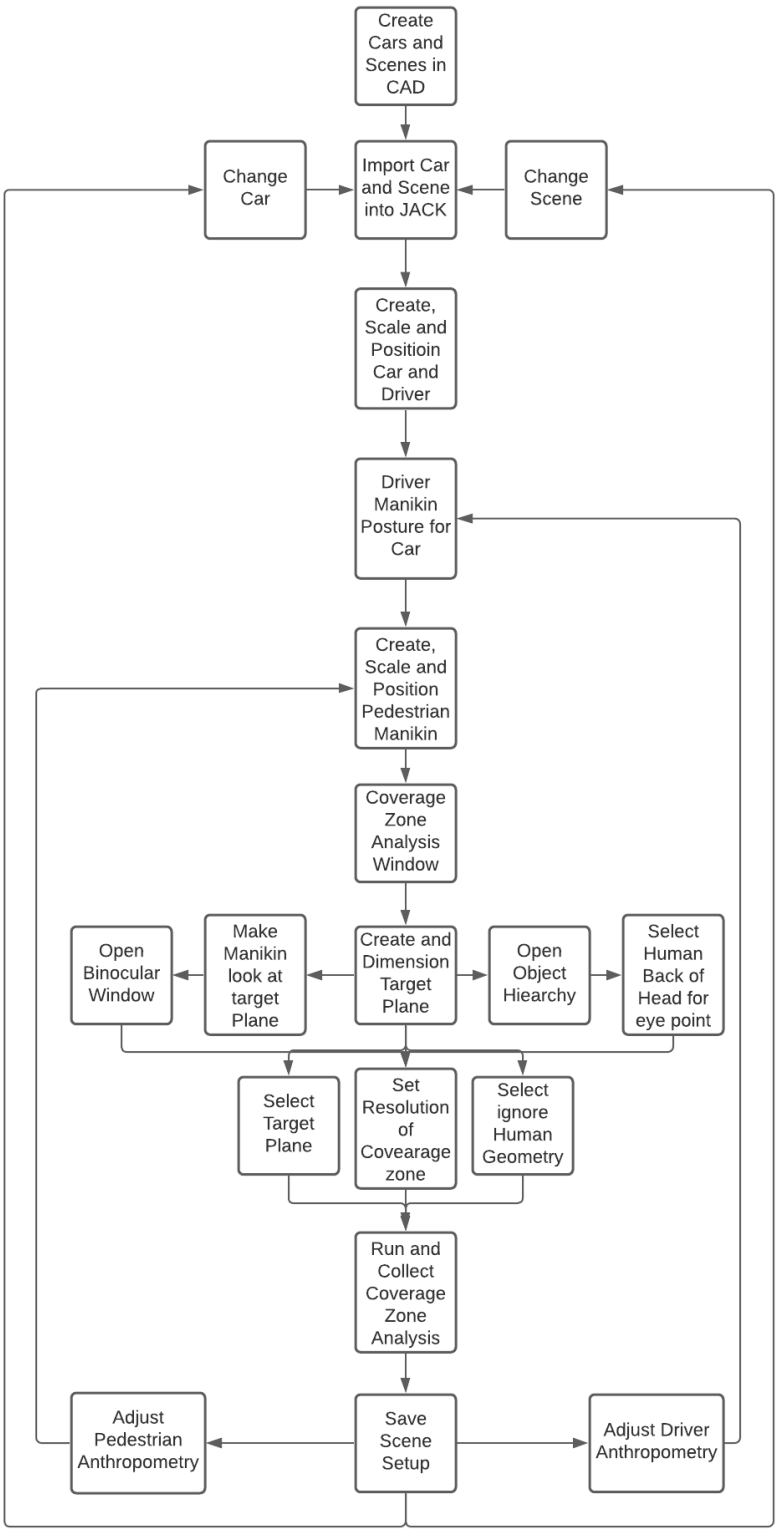

Figure A.1: Proof of concept Work Flow for Simulation

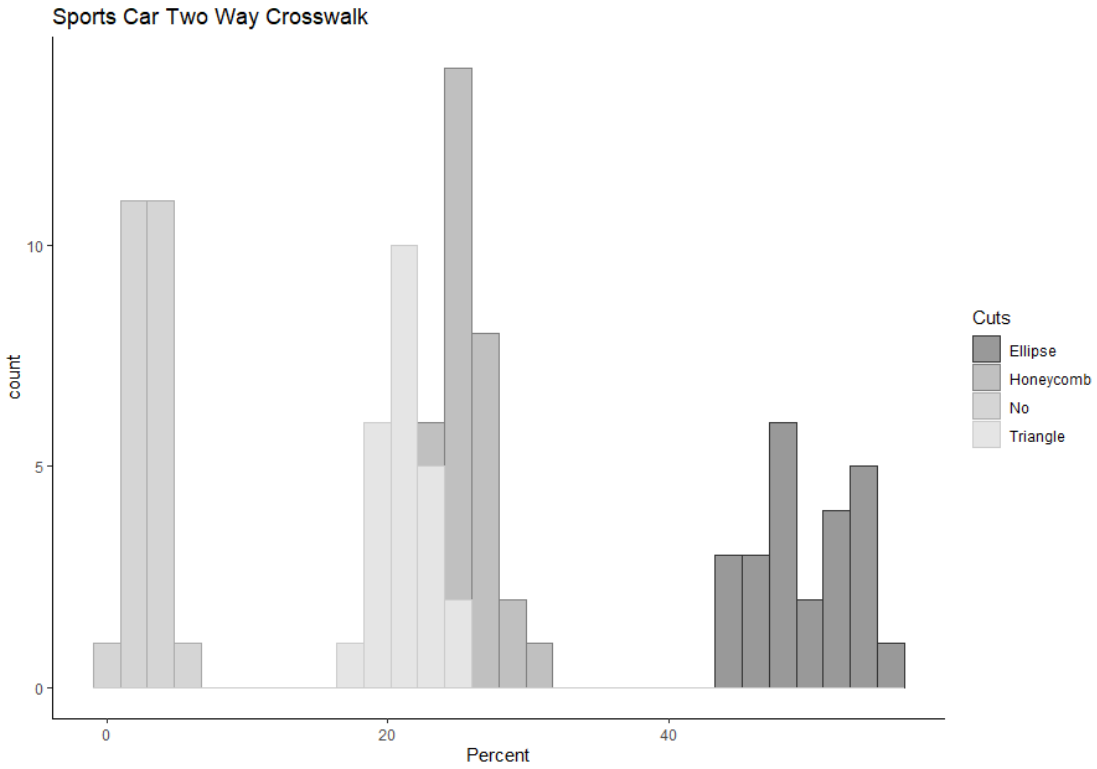

Figure A.2: Sports Car Crosswalk Histogram

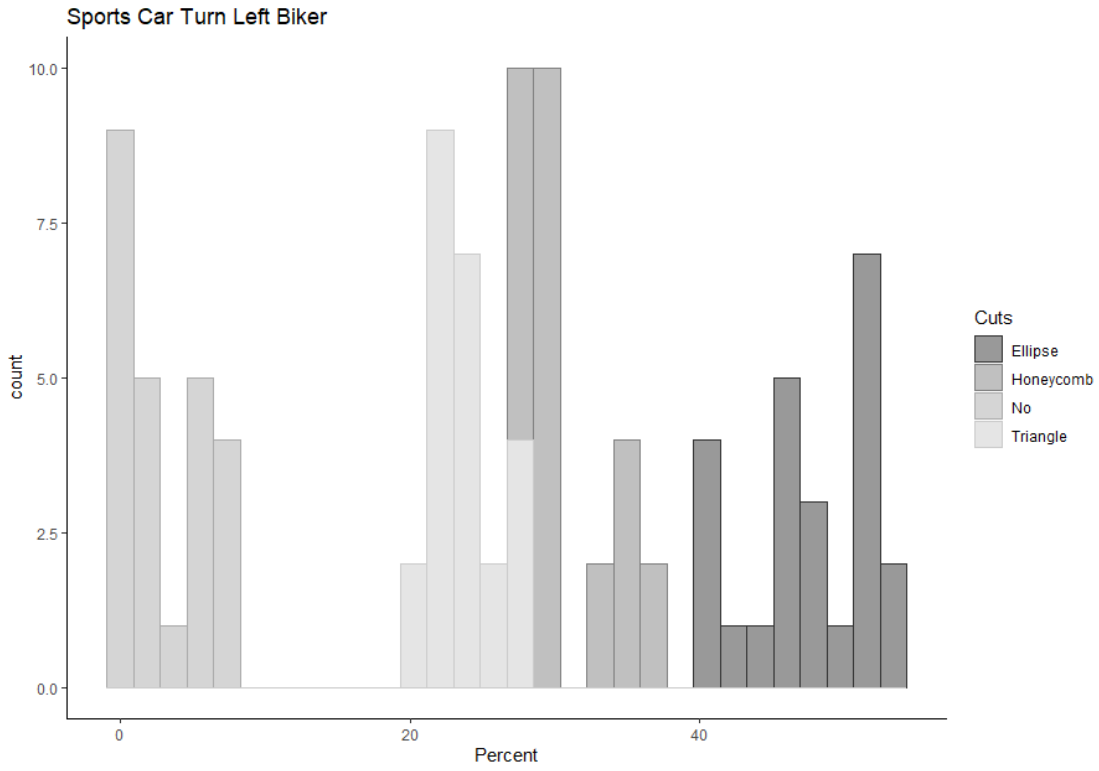

Figure A.3: Sports Car Turning Left Histogram

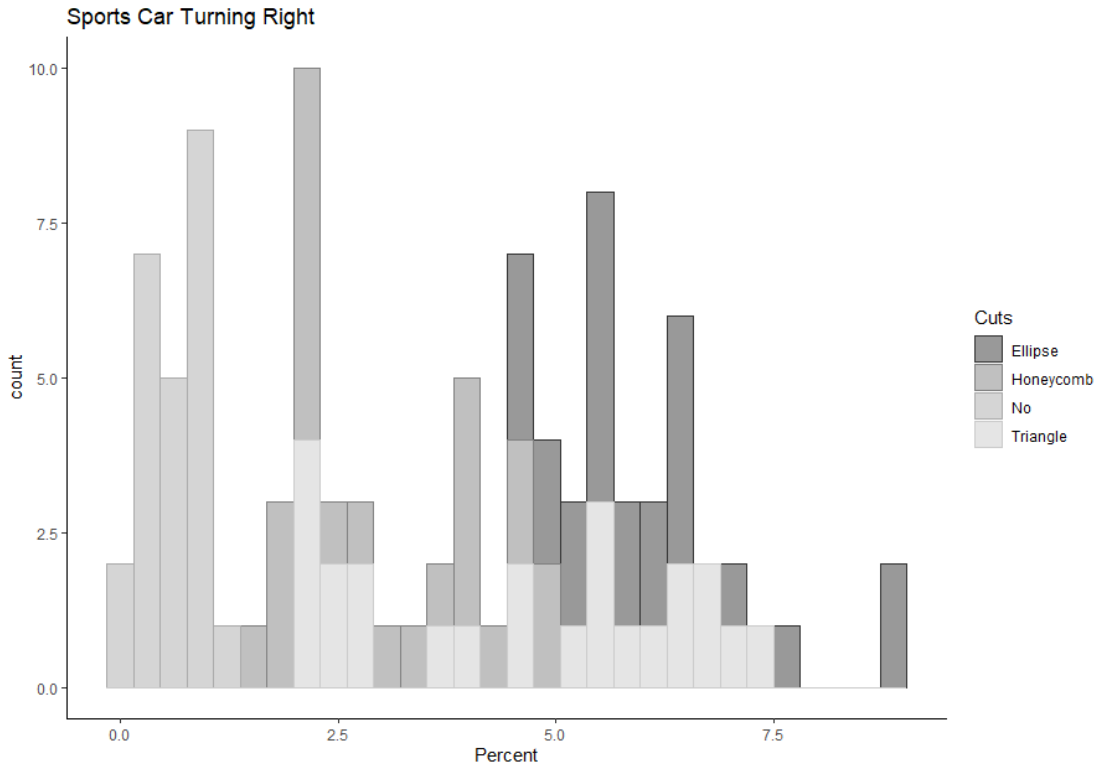

Figure A.4: Sports Car Turning Right Histogram

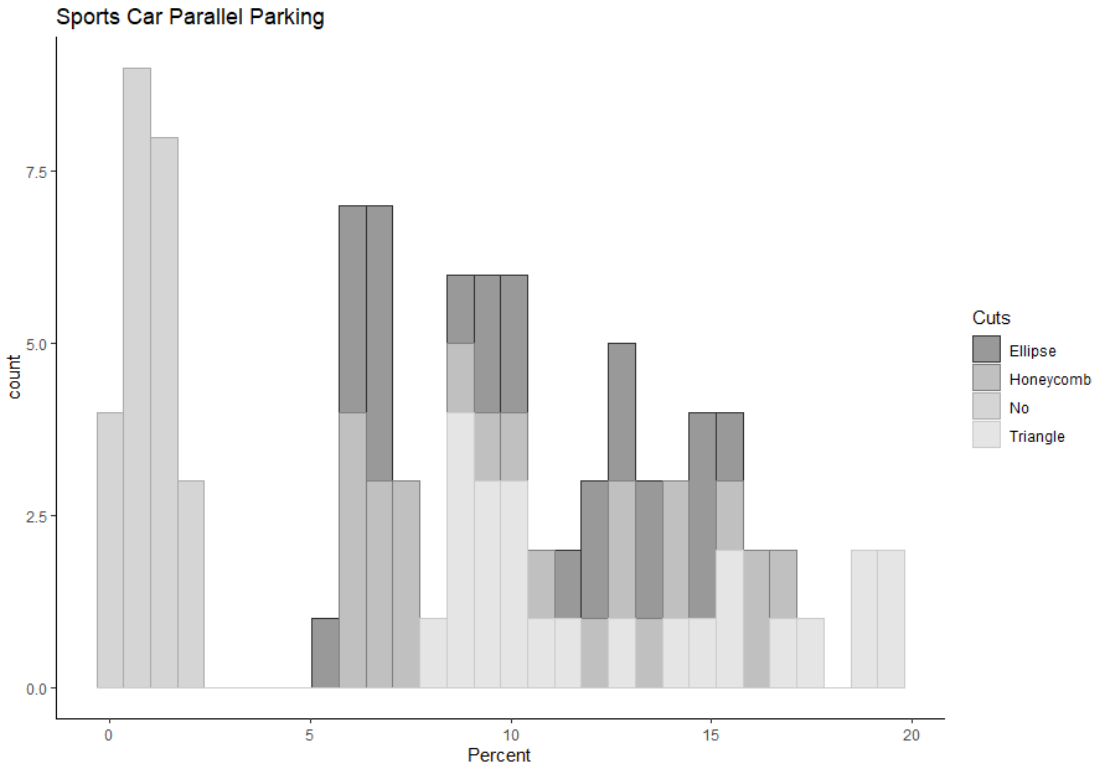

Figure A.5: Sports Car Parallel Parking Histogram

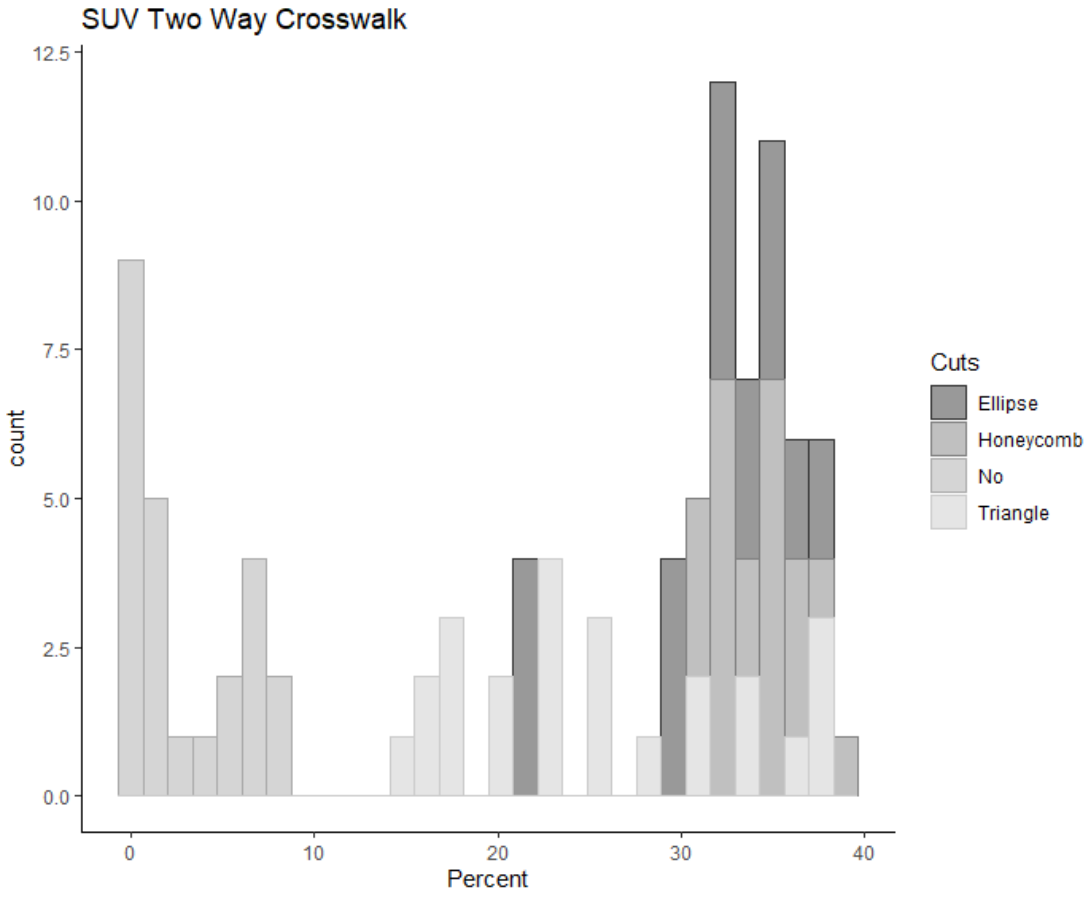

Figure A.6: SUV Crosswalk Histogram

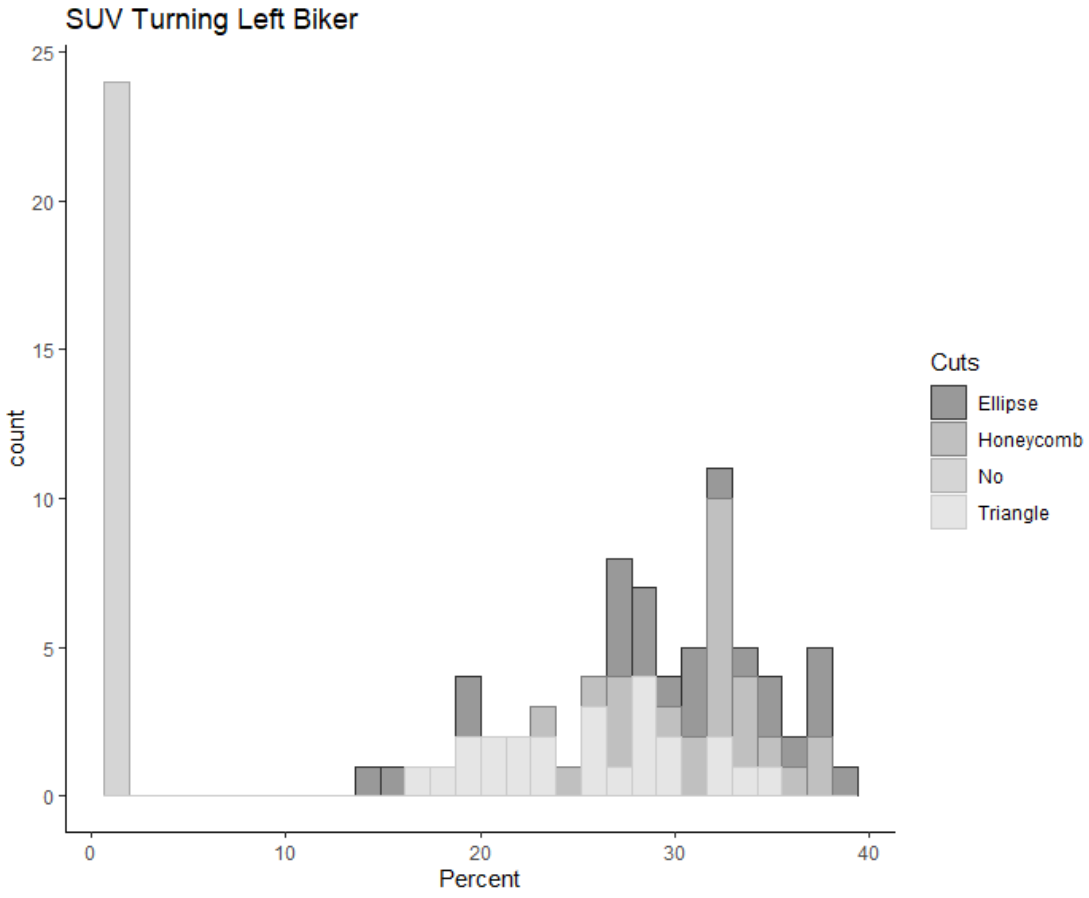

Figure A.7: SUV Turning Left Histogram

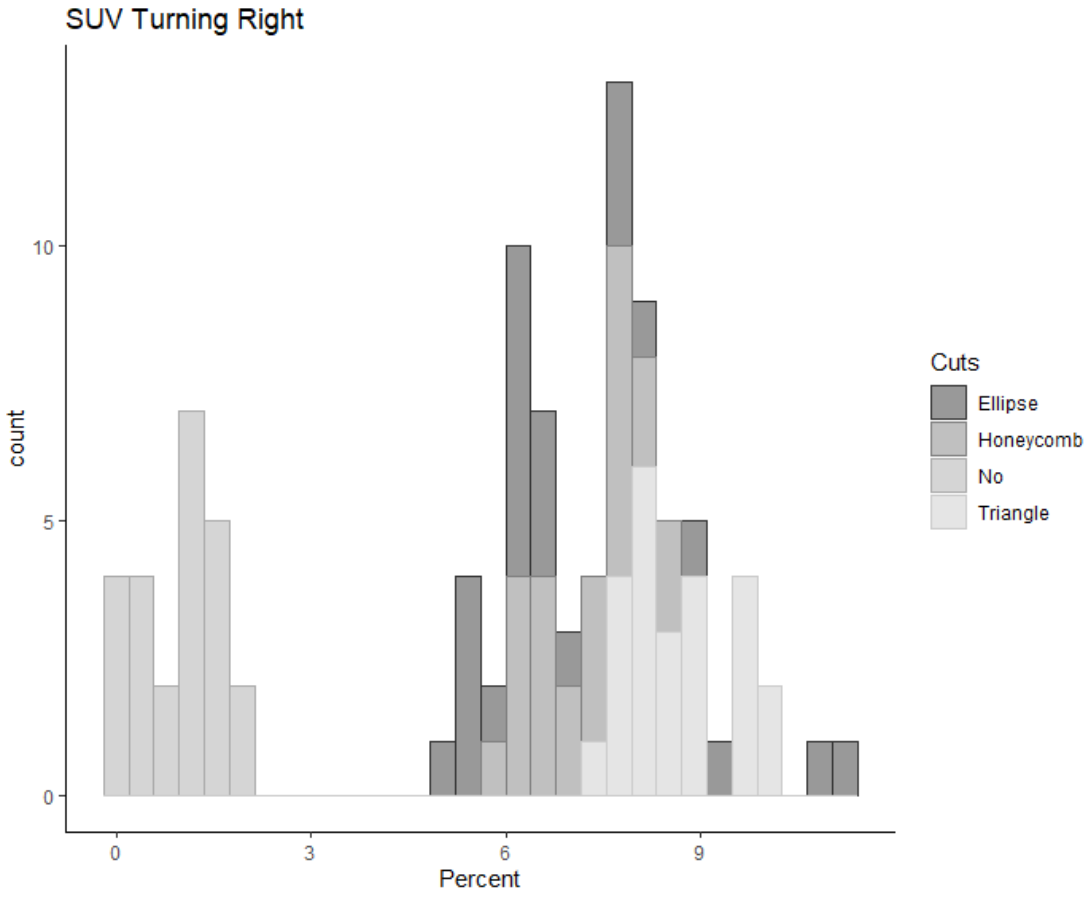

Figure A.8: SUV Turning Right Histogram

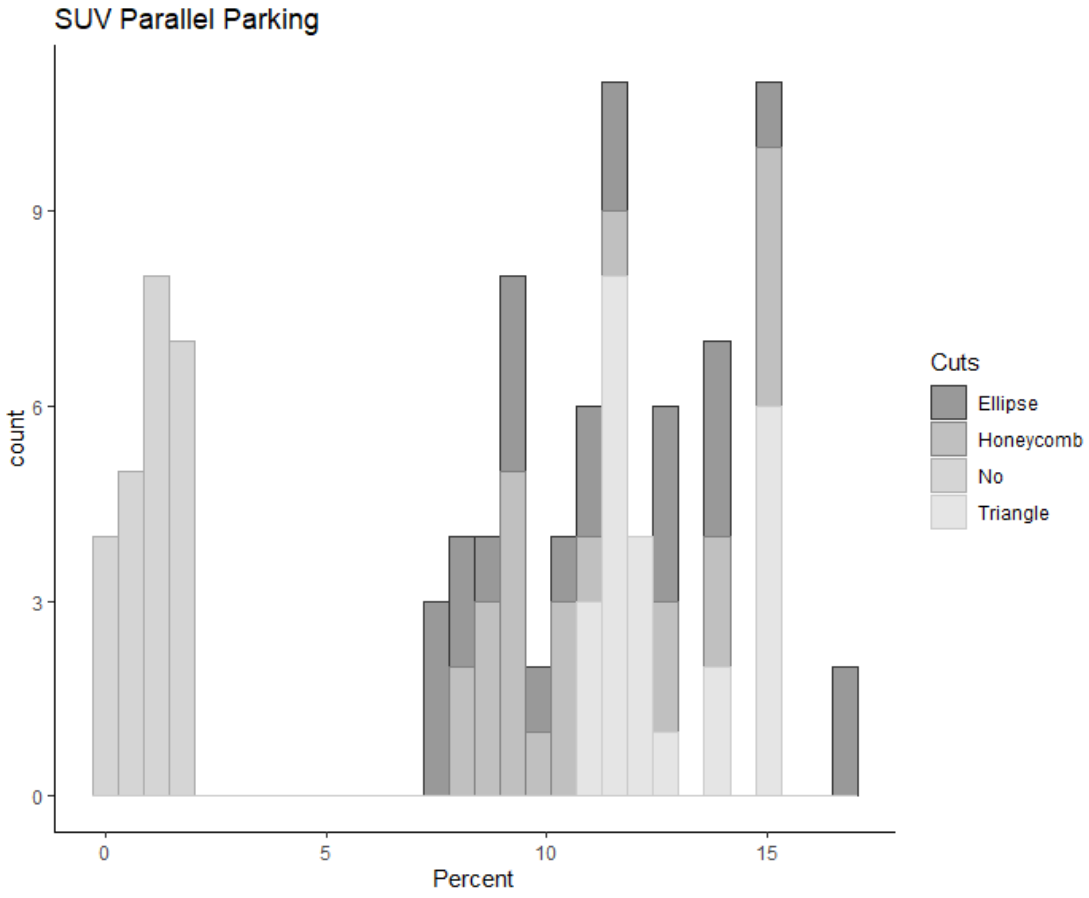

Figure A.9: SUV Parallel Parking Histogram

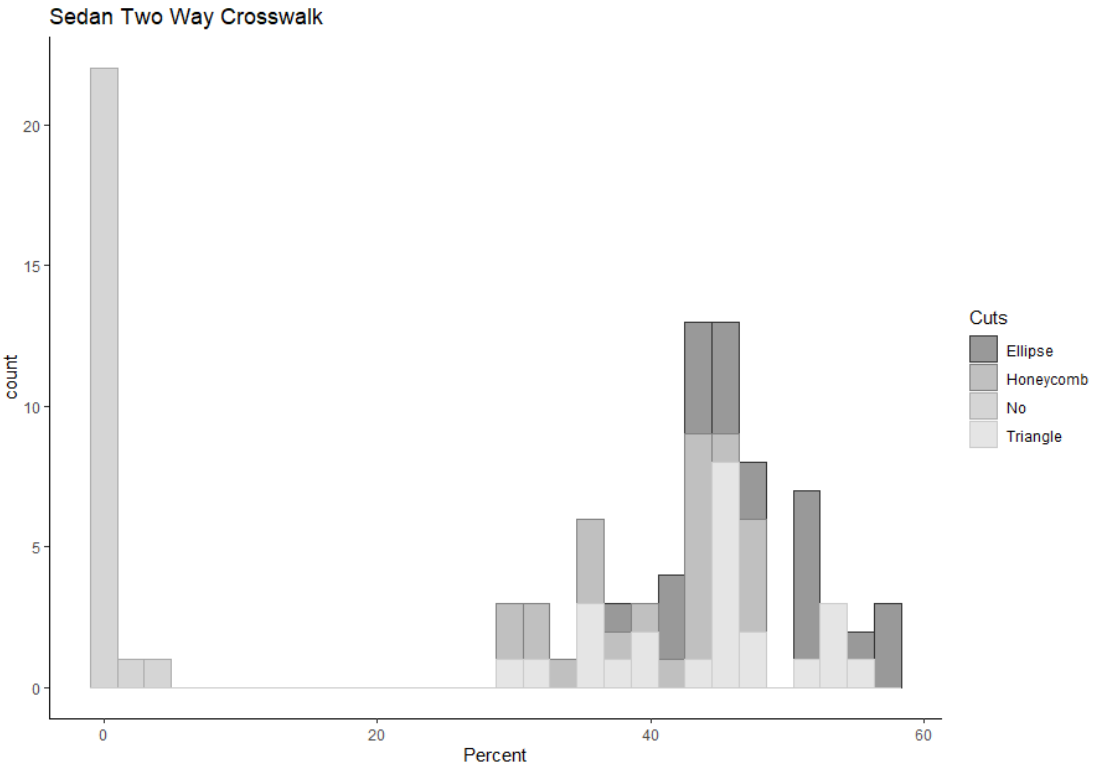

Figure A.10: Sedan Crosswalk Histogram

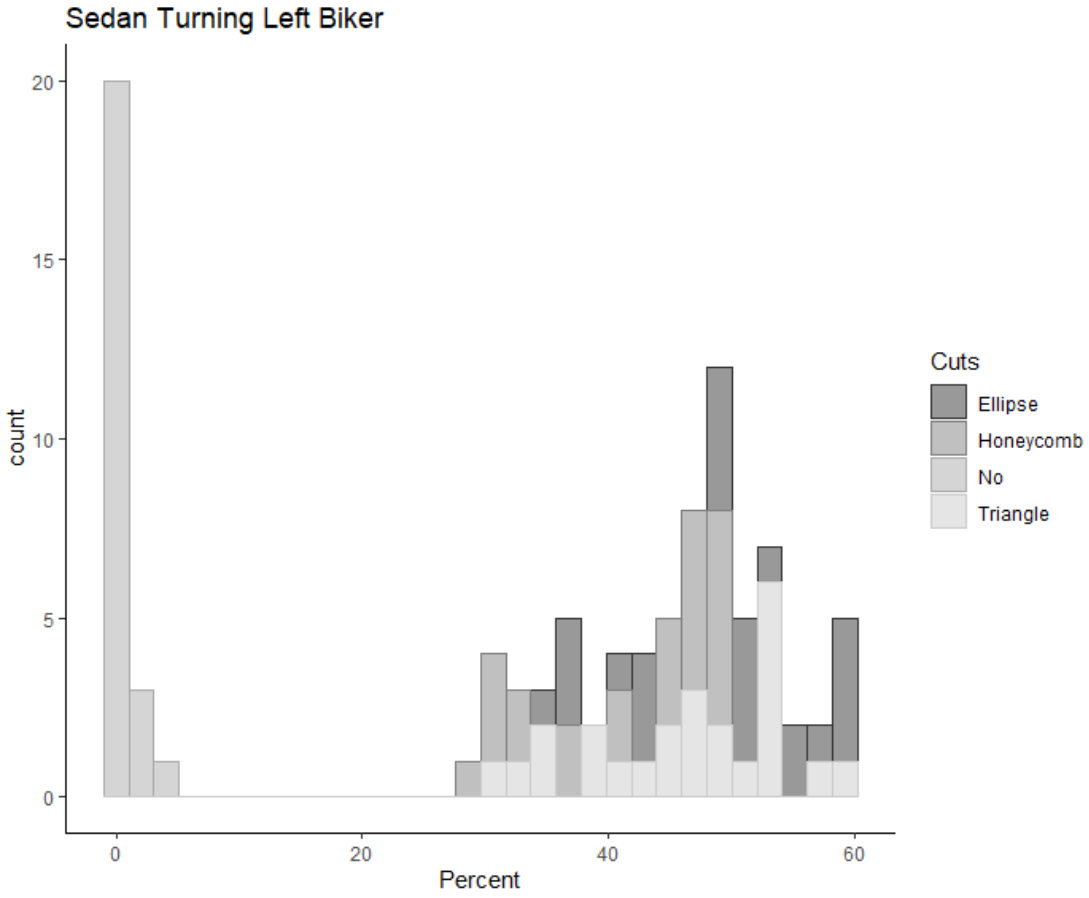

Figure A.11: Sedan Turning Left Histogram

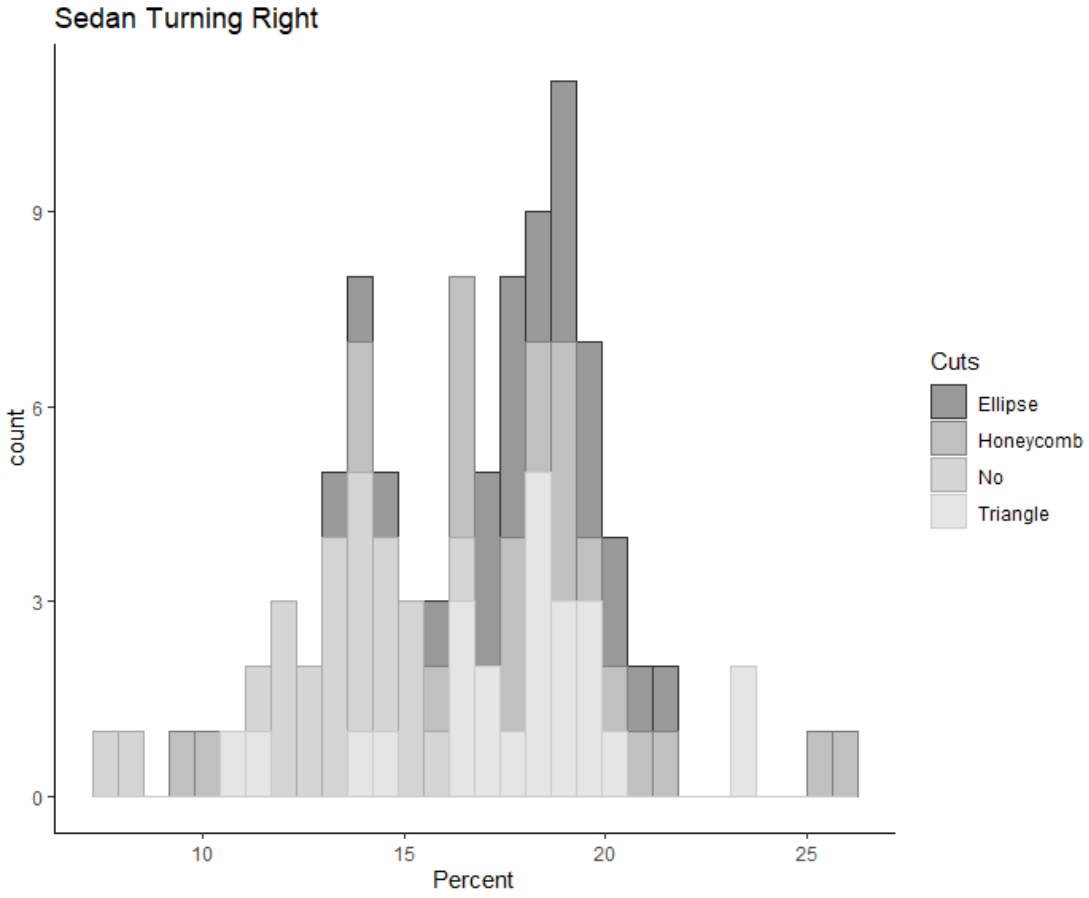

Figure A.12: Sedan Turning Right Histogram

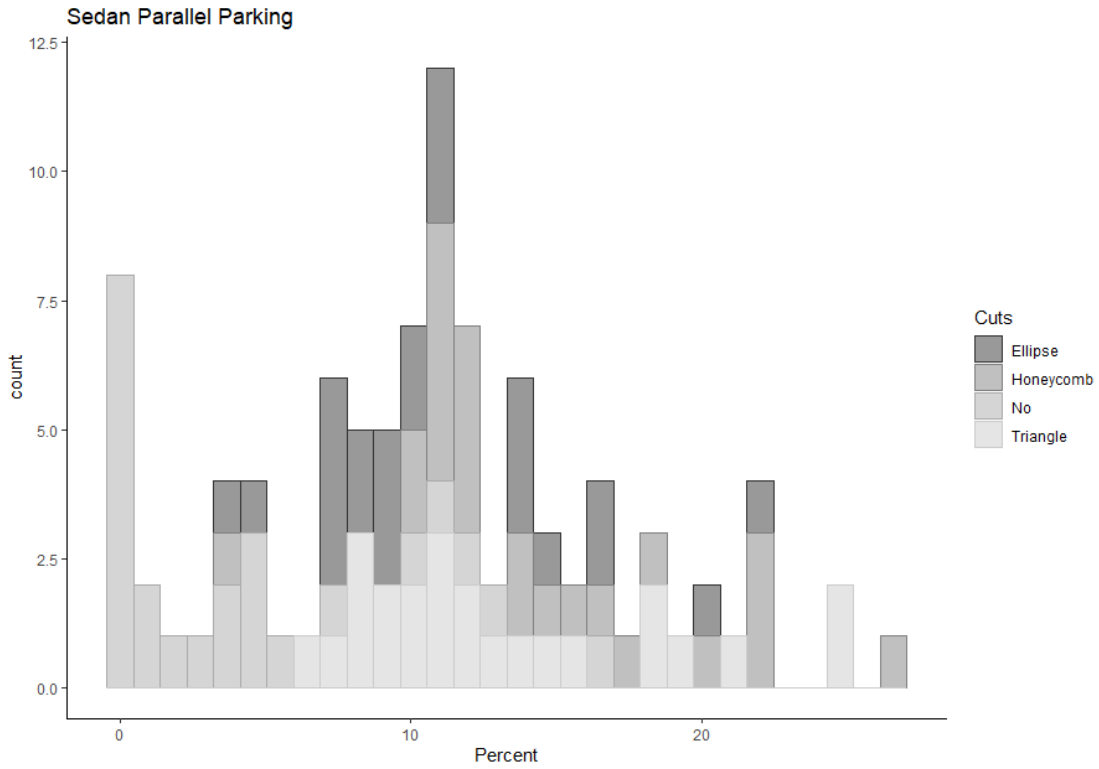

Figure A.13: Sedan Parallel Parking Histogram

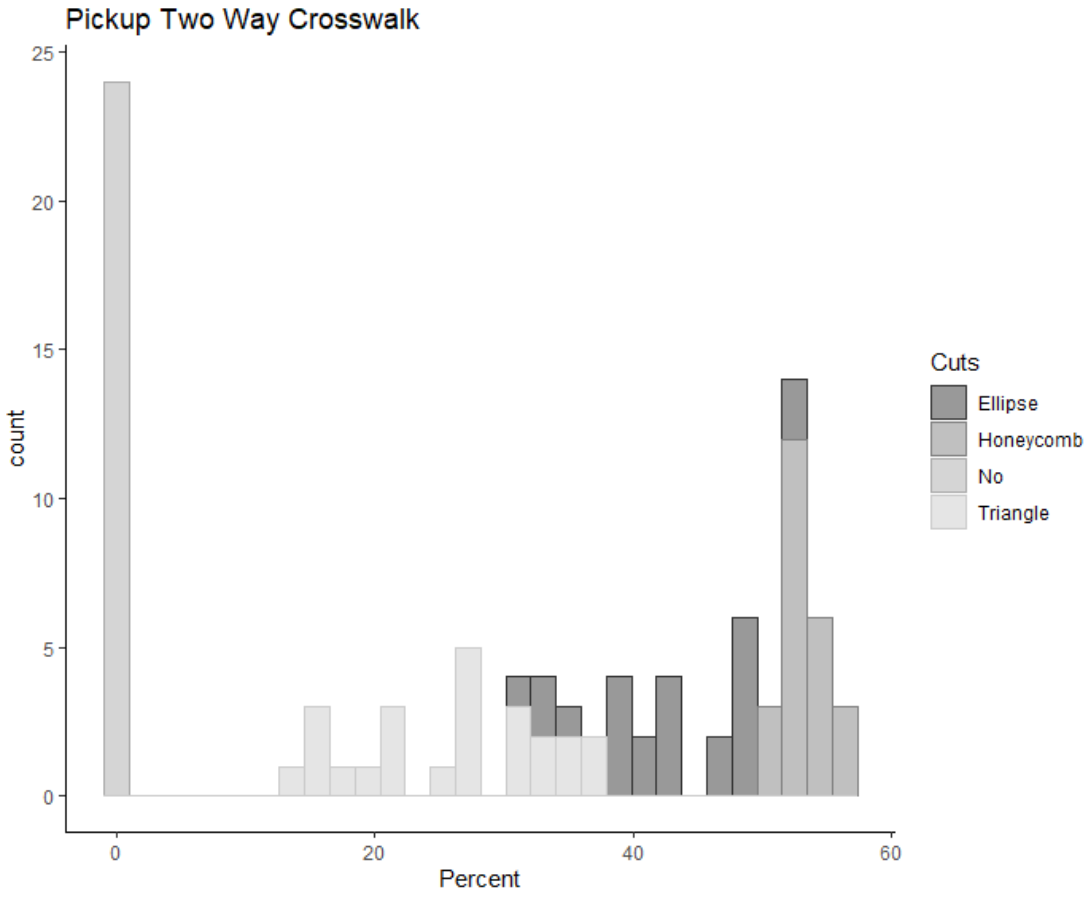

Figure A.14: Pickup Crosswalk Histogram

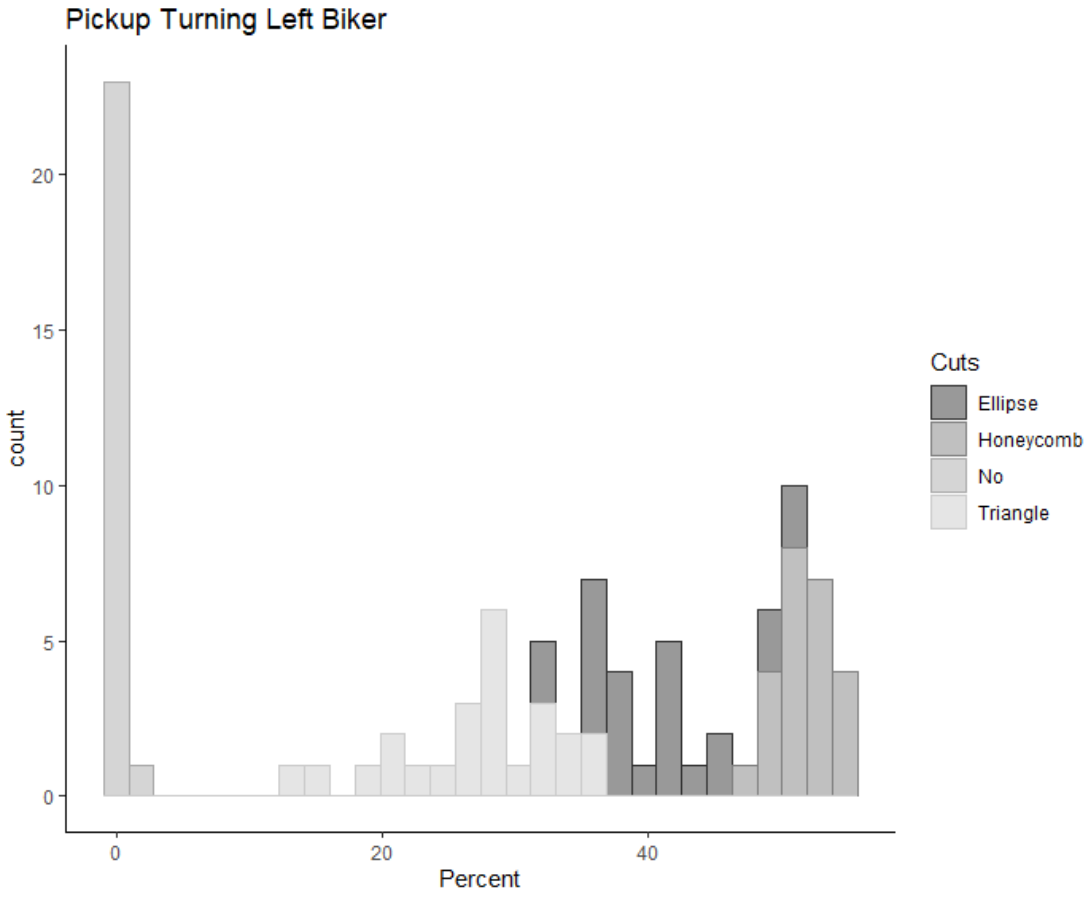

Figure A.15: Pickup Turning Left Histogram

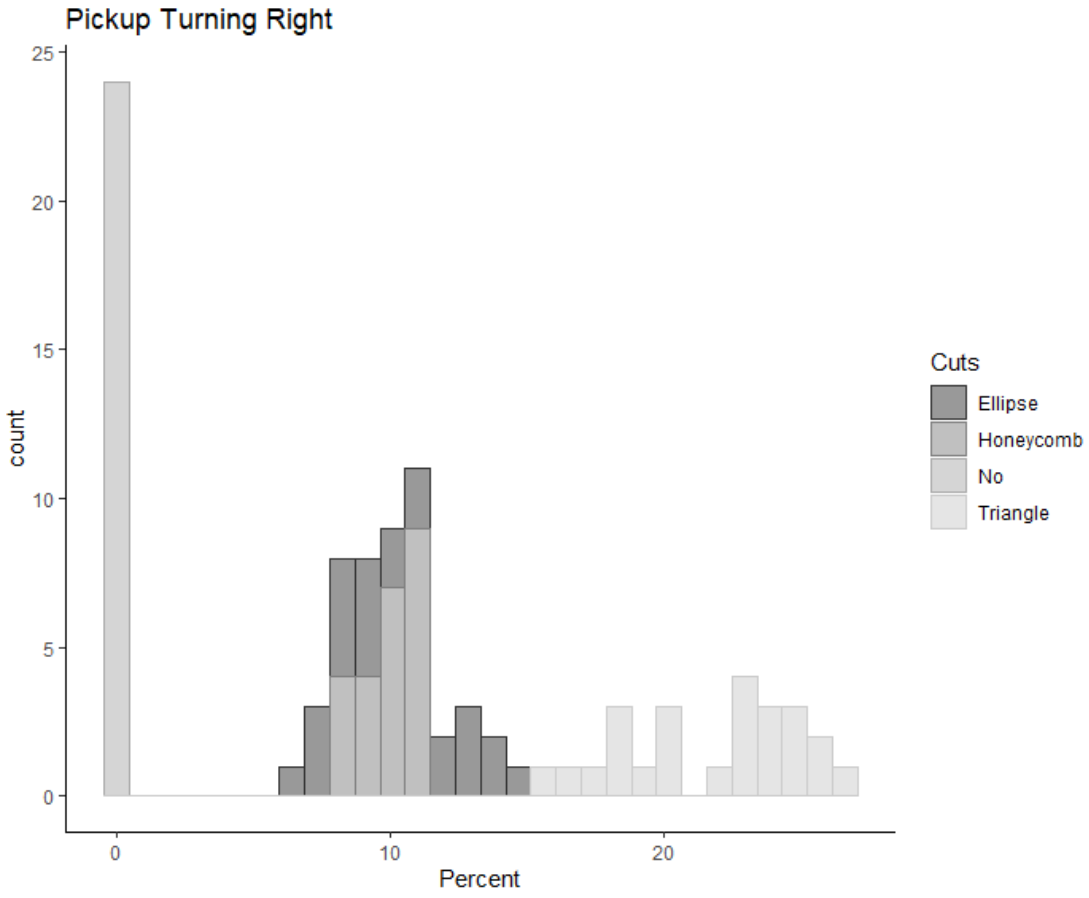

Figure A.16: Pickup Turning Right Histogram

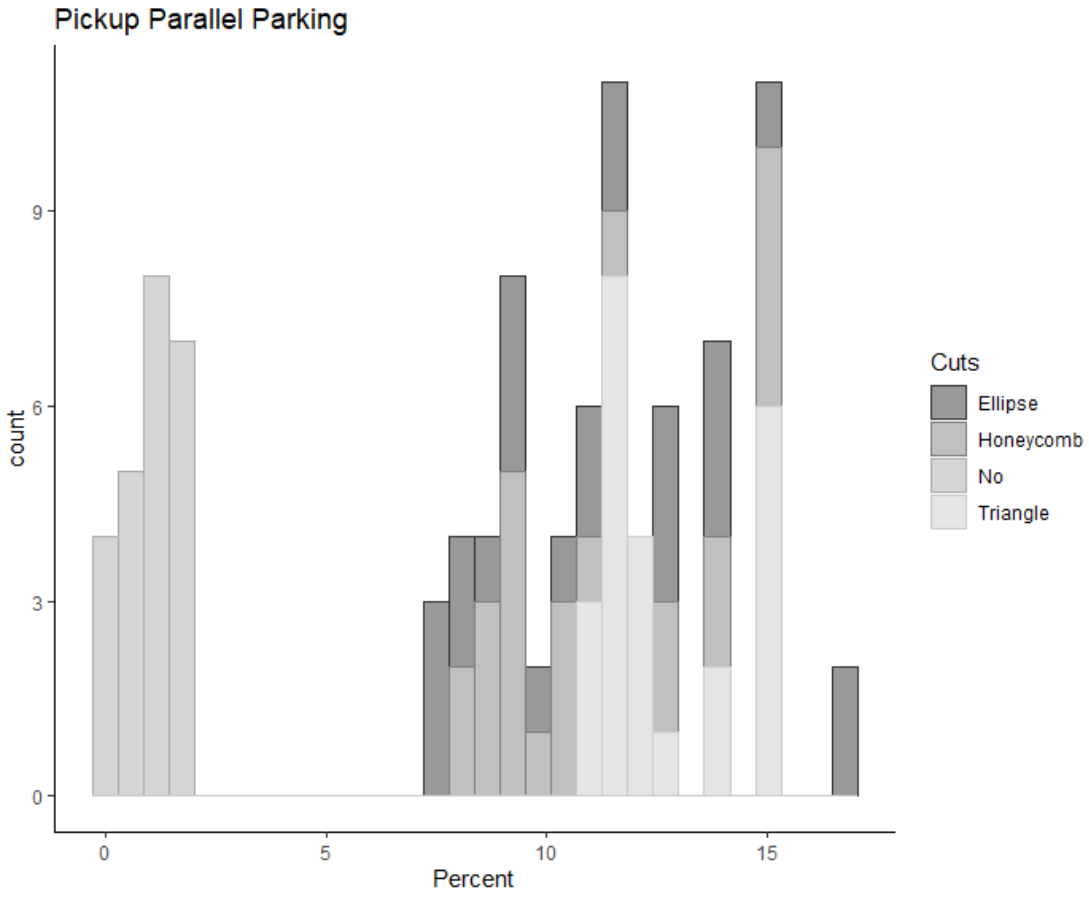

Figure A.17: Pickup Parallel Parking Histogram

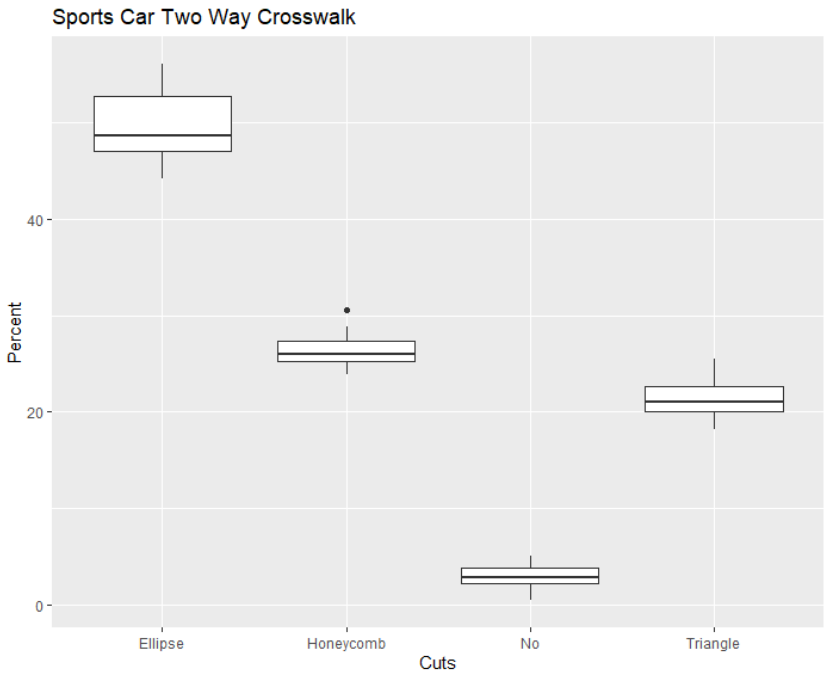

Figure A.18: Sports Car Crosswalk Box Plot

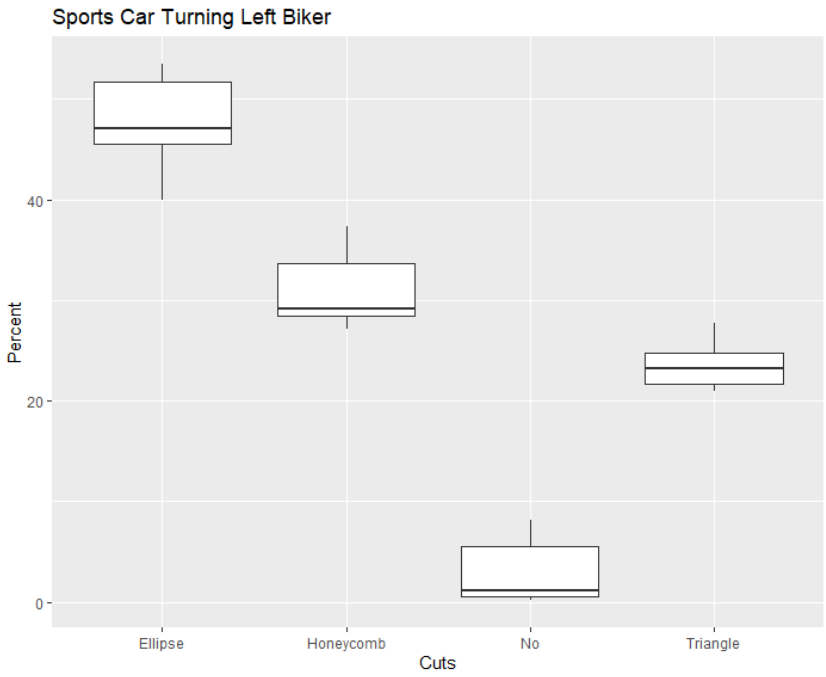

Figure A.19: Sports Car Turning Left Box Plot

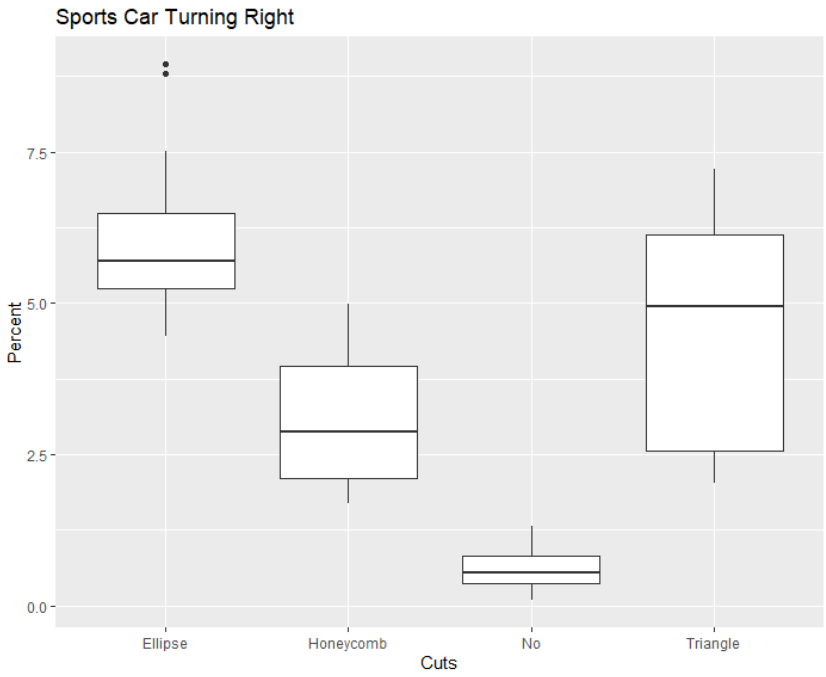

Figure A.20: Sports Car Turning Right Box Plot

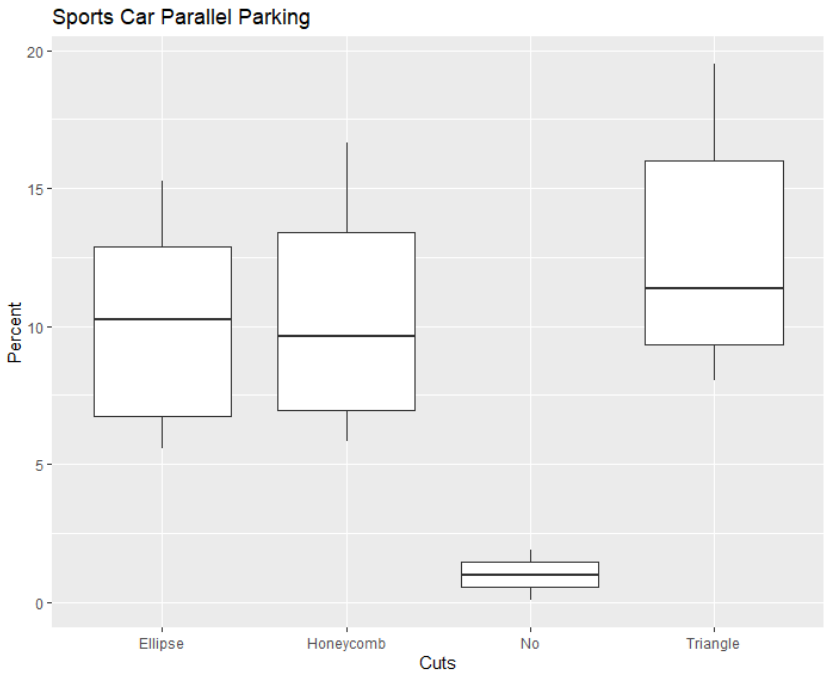

Figure A.21: Sports Car Parallel Parking Box Plot

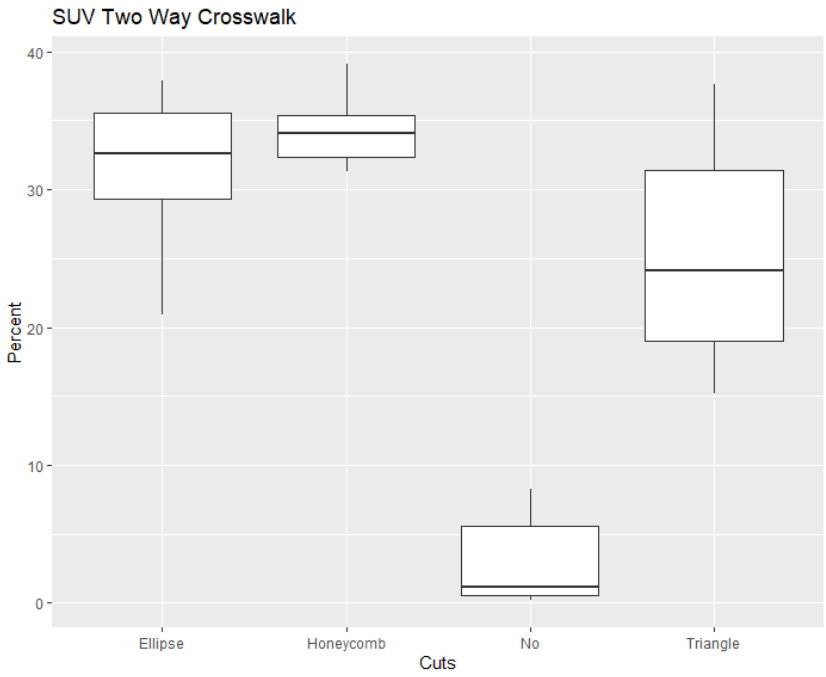

Figure A.22: SUV Crosswalk Box Plot

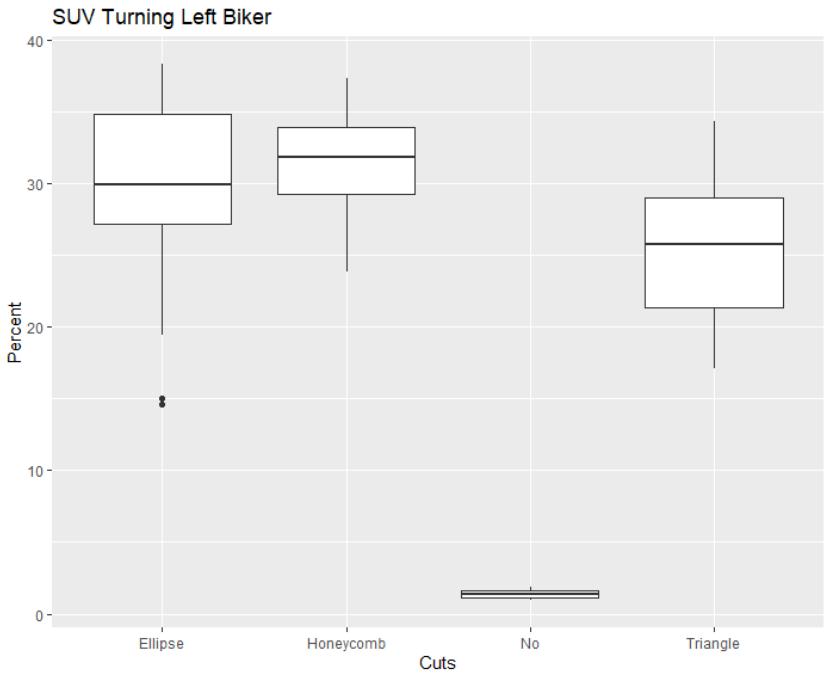

Figure A.23: SUV Turning Left Box Plot

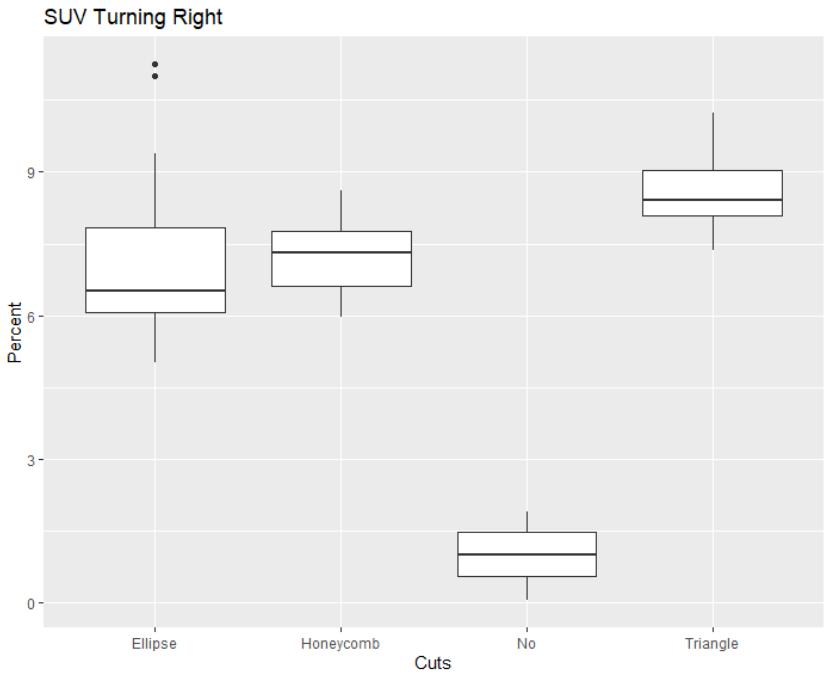

Figure A.24: SUV Turning Right Box Plot

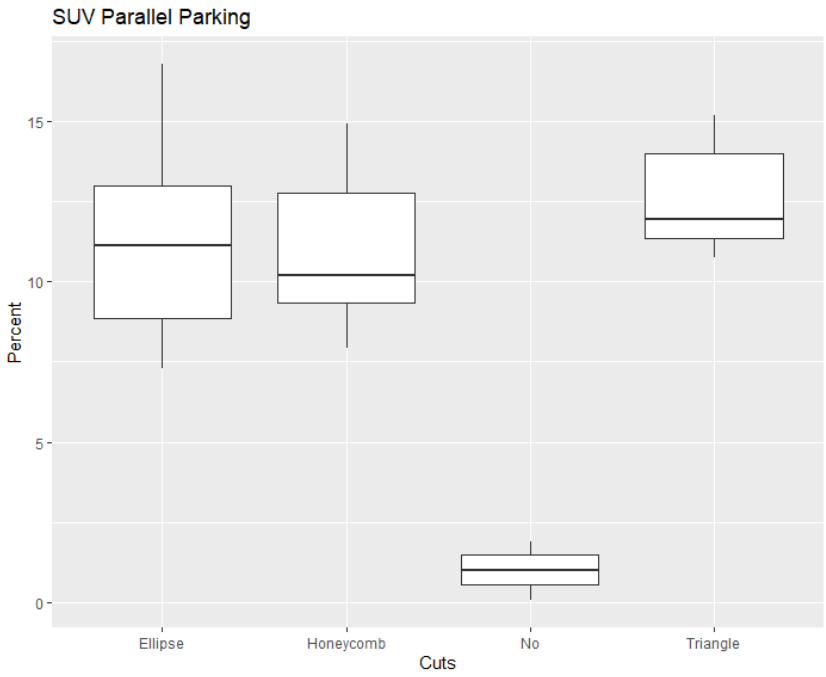

Figure A.25: SUV Parallel Parking Box Plot

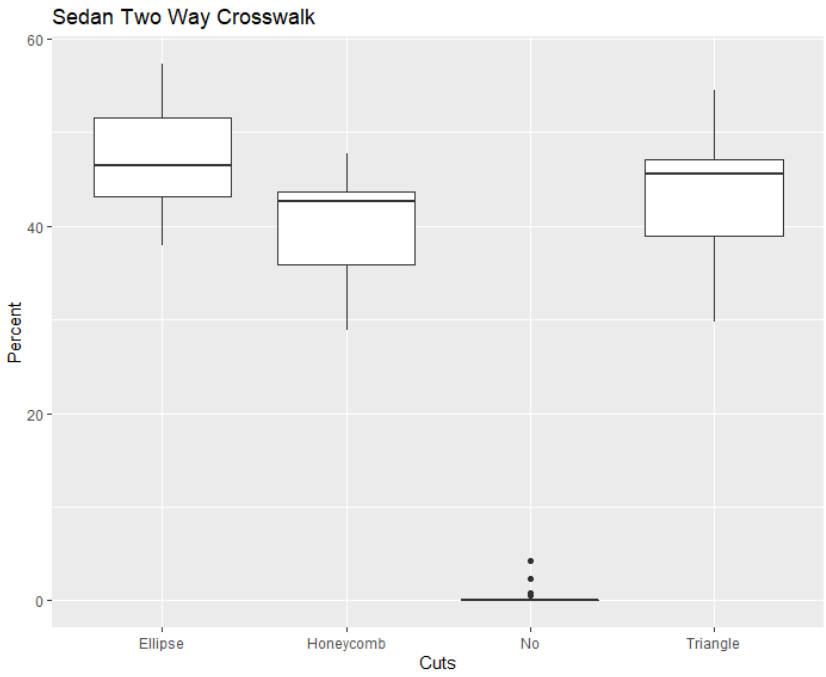

Figure A.26: Sedan Crosswalk Box Plot

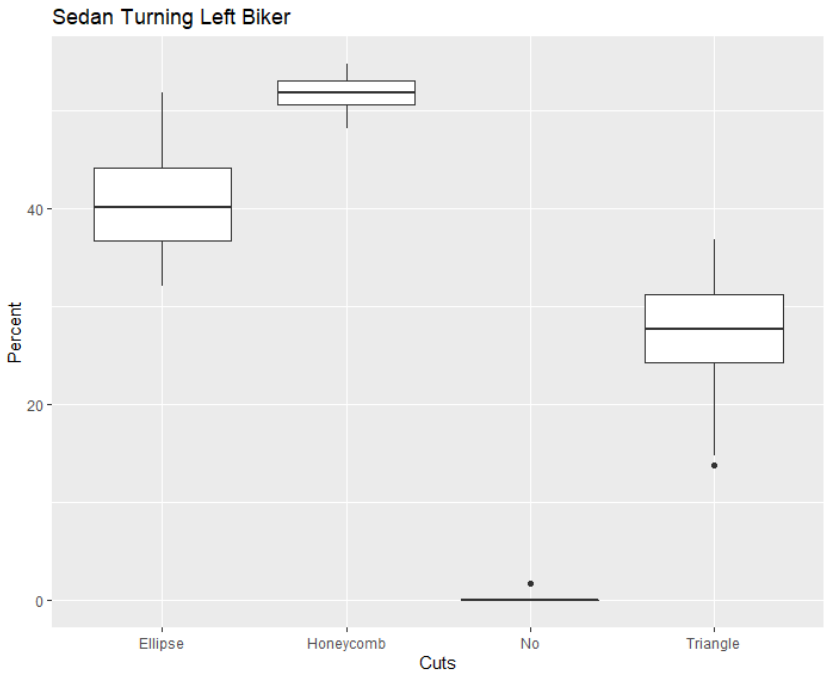

Figure A.27: Sedan Turning Left Box Plot

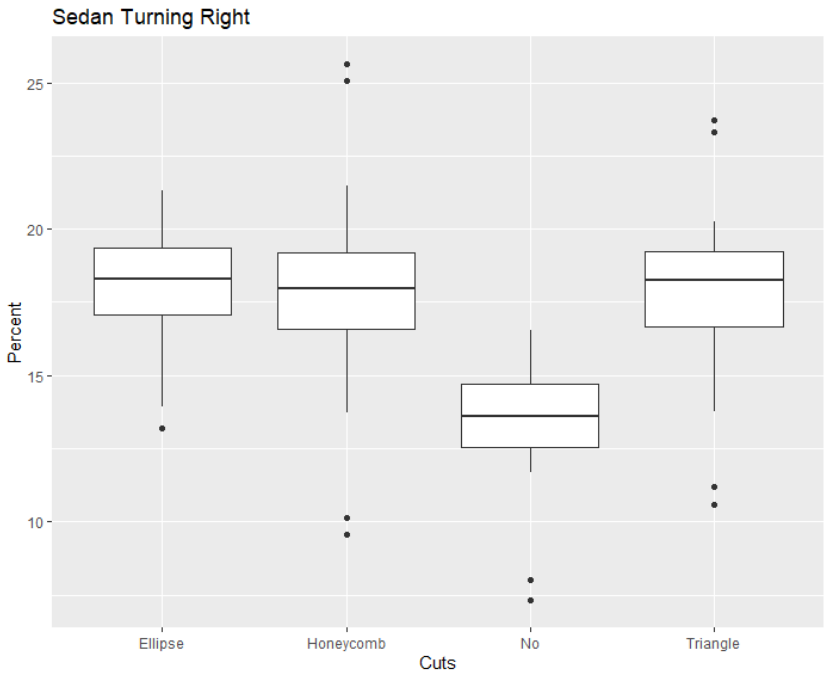

Figure A.28: Sedan Turning Right Box Plot

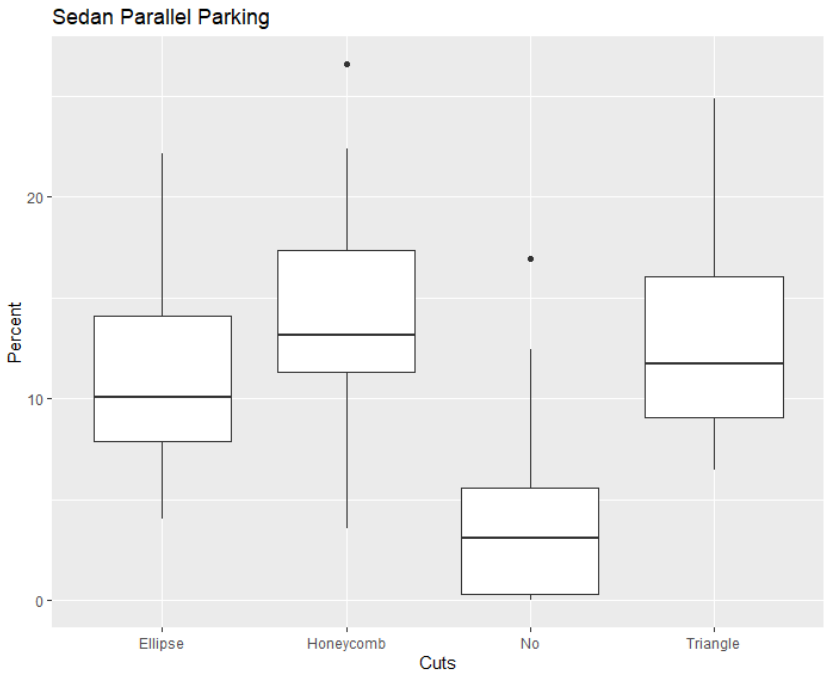

Figure A.29: Sedan Parallel Parking Box Plot

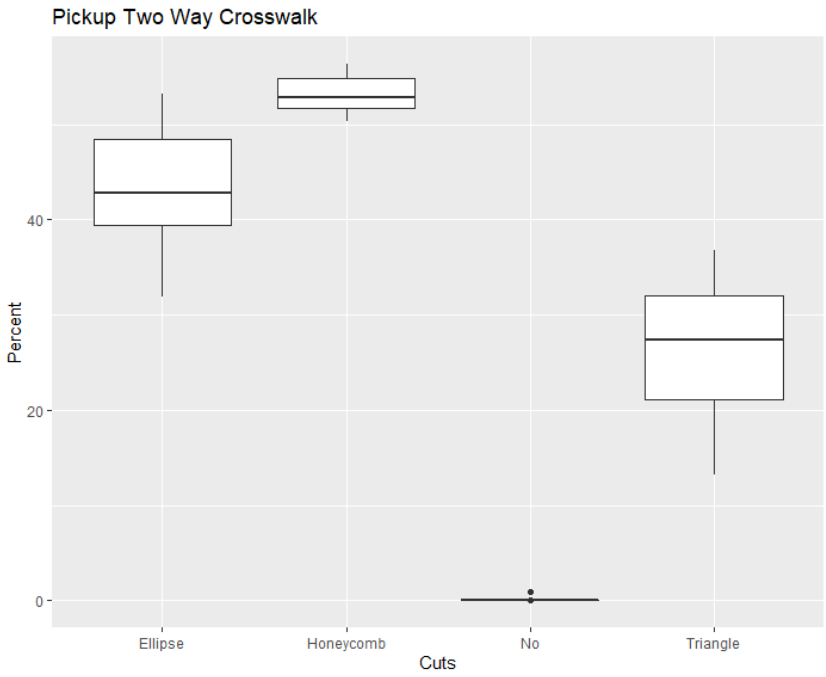

Figure A.30: Pickup Crosswalk Box Plot

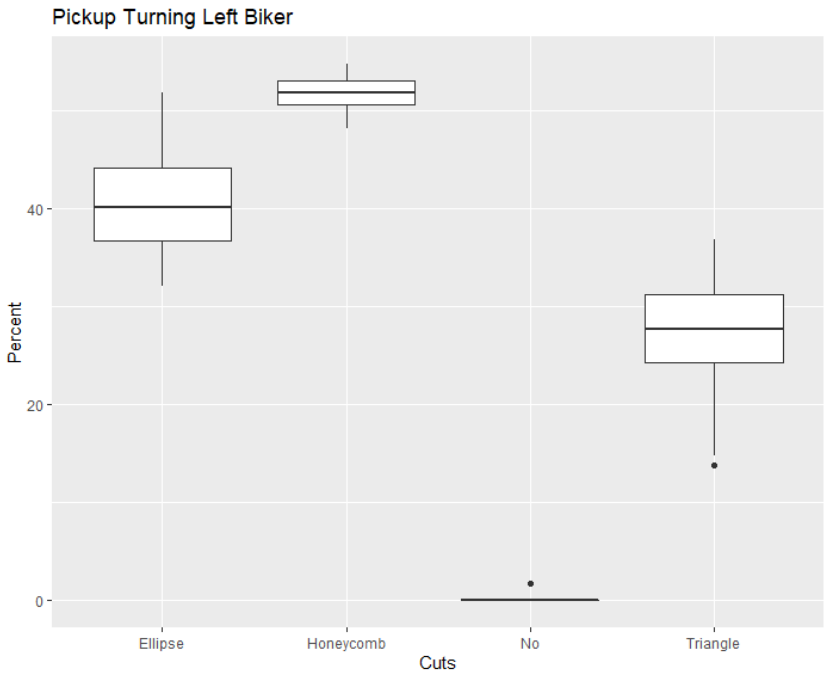

Figure A.31: Pickup Turning Left Box Plot

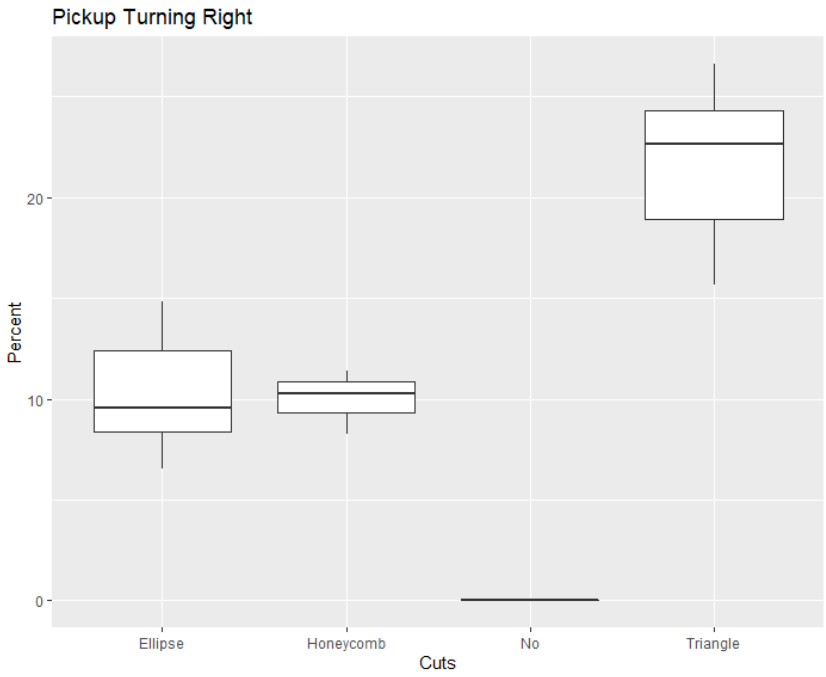

Figure A.32: Pickup Turning Right Box Plot

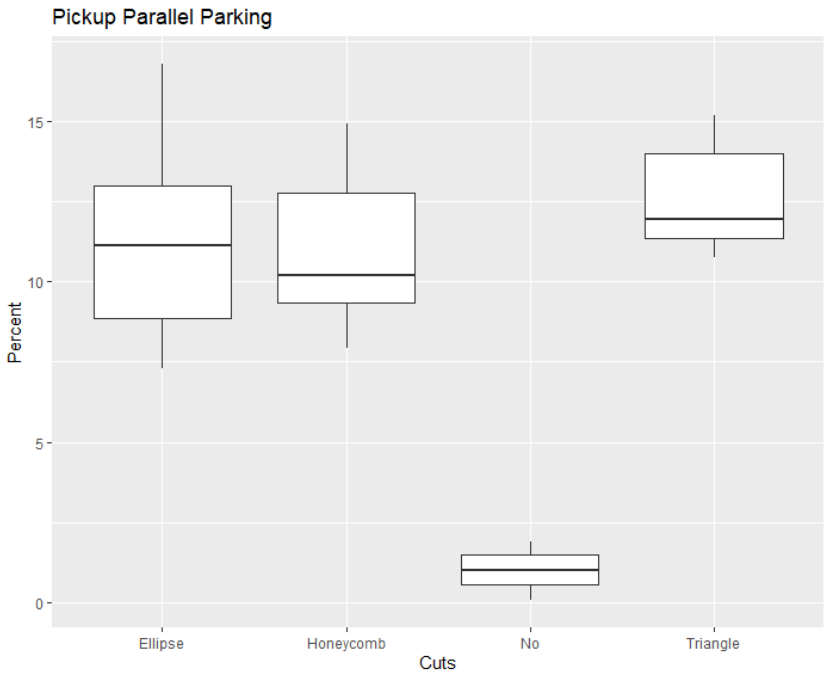

Figure A.33: Pickup Parallel Parking Box Plot

Table A.1: Sports Car General Statistics

Sports Car - General Statistics						
Scene	**Cuts**	**Count**	**Mean**	**sd**	**Median**	**IQR**
Turning Left	No	24	2.95	2.95	1.14	5.01
	Ellipse	24	47.6	4.37	47.1	6.18
	Triangle	24	23.6	2.2	23.3	2.98
	Honeycomb	24	30.8	3.14	29.2	5.15
Two Lane Highway	No	24	2.92	1.27	2.8	1.6
	Ellipse	24	49.6	3.66	48.7	5.63
	Triangle	24	21.4	1.89	21.1	2.59
	Honeycomb	24	26.3	1.54	25.9	2.12
Turning Right	No	24	0.6	0.32	0.54	0.45
	Ellipse	24	6.02	1.17	5.7	1.24
	Triangle	24	4.57	1.85	4.94	3.58
	Honeycomb	24	3.09	1.13	2.88	1.85
Parallel Parking	No	24	0.98	0.58	1	0.92
	Ellipse	24	10.2	3.35	10.2	6.15
	Triangle	24	12.8	4	11.4	6.65
	Honeycomb	24	10.4	3.74	9.64	6.45

Table A.2: SUV General Statistics

SUV - General Statistics						
Scene	**Cuts**	**Count**	**Mean**	**sd**	**Median**	**IQR**
Turning Left	No	24	1.39	0.3	1.38	0.47
	Ellipse	24	29.5	6.82	29.9	7.6
	Triangle	24	25.6	5.1	25.8	7.68
	Honeycomb	24	31.3	3.72	31.9	4.68
Two Lane Highway	No	24	2.95	1.27	2.8	1.6
	Ellipse	24	31.4	3.66	48.7	5.63
	Triangle	24	25.5	1.89	21.1	2.59
	Honeycomb	24	34.1	1.54	25.9	2.12
Turning Right	No	24	0.98	0.58	1	0.92
	Ellipse	24	7.05	1.69	6.51	1.76
	Triangle	24	8.64	0.83	8.41	0.95
	Honeycomb	24	7.23	0.75	7.32	1.14
Parallel Parking	No	24	0.98	0.58	1	0.92
	Ellipse	24	11.1	2.86	11.1	4.13
	Triangle	24	12.6	1.56	11.9	2.62
	Honeycomb	24	11	2.4	10.2	3.46

Table A.3: Sedan General Statistics

Sedan - General Statistics						
Scene	**Cuts**	**Count**	**Mean**	**sd**	**Median**	**IQR**
Turning Left	No	24	0.57	1.13	0.08	0.2
	Ellipse	24	48.9	7.76	50.2	12
	Triangle	24	46.3	8.01	47	12
	Honeycomb	24	41.9	7.33	45.8	12
Two Lane Highway	No	24	0.37	0.97	0	0
	Ellipse	24	47.8	5.58	46.4	8.4
	Triangle	24	44	6.98	45.6	8.2
	Honeycomb	24	40	5.83	42.7	7.7
Turning Right	No	24	13.3	2.14	13.6	2.2
	Ellipse	24	18.1	2.05	18.6	2.3
	Triangle	24	17.7	3.08	18.2	2.6
	Honeycomb	24	17.8	3.71	18	2.6
Parallel Parking	No	24	4.35	4.81	3.08	5.3
	Ellipse	24	11.2	4.52	10.1	6.2
	Triangle	24	13.3	5.37	11.8	7
	Honeycomb	24	14.6	5.18	13.1	6

Table A.4: Pickup General Statistics

Pickup - General Statistics						
Scene	**Cuts**	**Count**	**Mean**	**sd**	**Median**	**IQR**
Turning Left	No	24	0.0075	0.37	0	0
	Ellipse	24	40.9	5.6	40.1	7.43
	Triangle	24	27.1	5.98	27.7	6.92
	Honeycomb	24	51.7	1.89	51.7	2.45
Two Lane Highway	No	24	0.0417	0.18	0	0
	Ellipse	24	43.1	6.15	42.8	8.93
	Triangle	24	26.2	7.42	27.3	11
	Honeycomb	24	53.2	1.76	52.8	3.03
Turning Right	No	24	0	0	0	0
	Ellipse	24	10.2	2.46	9.55	4.07
	Triangle	24	21.9	3.15	22.6	5.38
	Honeycomb	24	10.1	0.96	10.3	1.54
Parallel Parking	No	24	0.975	0.58	1	0.92
	Ellipse	24	11.1	2.86	11.1	4.13
	Triangle	24	12.6	1.56	11.9	2.62
	Honeycomb	24	11	2.4	10.2	3.46